

1 **The inositol-3-phosphate synthase biosynthetic enzyme has distinct catalytic and**
2 **metabolic roles**

3

4

5 Anna D. Frej^a, Jonathan Clark^b, Caroline Le Roy^c, Sergio Lilla^d, Peter Thomason^d, Grant P.

6 Otto^a, Grant Churchill⁵, Robert Insall^d, Sandrine P. Claus^c, Phillip Hawkins^b, Len Stephens^b

7 and Robin S.B. Williams^{a#}

8

9 Centre for Biomedical Sciences, School of Biological Sciences, Royal Holloway University

10 of London, Egham, Surrey, UK^a; The Babraham Institute, Cambridge, Cambridgeshire, UK^b;

11 Department of Food and Nutritional Sciences, The University of Reading, Reading,

12 Berkshire, UK^c. CRUK Beatson Institute for Cancer Research, Glasgow, UK⁴. Department of

13 Pharmacology, University of Oxford, Oxford, Oxfordshire, UK⁵

14

15 Running Head: Distinct catalytic and metabolic roles of Ino1

16

17 Address correspondence to Robin S.B. Williams, robin.williams@rhul.ac.uk.

18

19 Word count: Abstract 200

20 Material and Methods 7593

21 Intro/Results/Discussion/Legends 39951

22

23 **ABSTRACT**

24 Inositol levels, maintained by the biosynthetic enzyme inositol-3-phosphate synthase (Ino1), are
25 altered in a range of disorders including bipolar disorder and Alzheimer's disease. To date, most
26 inositol studies have focused on the molecular and cellular effects of inositol depletion without
27 considering Ino1 levels. Here we employ a simple eukaryote, *Dictyostelium*, to demonstrate
28 distinct effects of loss of Ino1 and inositol depletion. We show that loss of Ino1 results in
29 inositol auxotrophy that can only be partially rescued by exogenous inositol. Removal of
30 inositol supplementation from the *ino1* mutant results in a rapid 56% reduction in inositol
31 levels, triggering the induction of autophagy, reduced cytokinesis and substrate adhesion.
32 Inositol depletion also caused a dramatic generalised decrease in phosphoinositide levels that
33 was rescued by inositol supplementation. However, loss of Ino1 triggered broad metabolic
34 changes consistent with the induction of a catabolic state that was not rescued by inositol
35 supplementation. These data suggest a metabolic role for Ino1 independent of inositol
36 biosynthesis. To characterise this role, an Ino1 binding partner containing SEL1L1 domains
37 (Q54IX5) was identified with homology to mammalian macromolecular complex adaptor
38 proteins. Our findings therefore identify a new role for Ino1, independent of inositol
39 biosynthesis, with broad effects on cell metabolism.

40

41 **INTRODUCTION**

42 *Myo*-inositol, a stereoisomer of inositol, is present in a variety of cell types and is obtained from
43 three major sources: *de novo* synthesis from glucose-6-phosphate, sequential dephosphorylation
44 of phosphoinositides, or membrane transport from extracellular fluid (15). Disruption of inositol
45 homeostasis has been associated with a number of illnesses, including bipolar disorder
46 (3,4,61,76), Alzheimer's disease (2,41,68,74), bulimia (26), metabolic syndrome (39), diabetes

47 (30,52), and epilepsy (7). Understanding the cellular and metabolic changes resulting from
48 inositol depletion will provide insight into the mechanisms underlying these diseases.

49 Inositol-3-phosphate synthase (Ino1, EC 5.5.1.4) is crucial in the *de novo* biosynthesis of
50 inositol, as an isomerase that converts glucose-6-phosphate to inositol-3-phosphate, which is
51 then dephosphorylated to inositol (33)(Fig 1A). Inositol is an essential precursor of a large
52 family of phosphoinositides (14), with one of these, phosphoinositide 4,5 bisphosphate (PIP2),
53 used in the production of inositol phosphates. These molecules are important for a range of
54 cellular functions, including motility (42), activation of signal transduction pathways (18),
55 membrane trafficking and vesicular transport (15), protein secretion, and transcriptional
56 regulation (62). Despite these broad functions, few studies have compared the physiological
57 effects of reducing inositol levels and reducing Ino1 levels, therefore it remains unclear if these
58 two effects have distinct roles.

59 *Dictyostelium discoideum* is a single-celled eukaryote found in forest soils, where it survives by
60 consuming bacteria. *Dictyostelium* is used as a research model in a variety of disciplines
61 including biomedicine. We previously employed *Dictyostelium* in a 3Rs approach (animal
62 reduction, replacement and refinement) for biomedical research, to investigate the effects of
63 epilepsy treatments on modulating phosphoinositide signalling and seizure control (6,7) and the
64 effects of bipolar disorder treatments on the level of inositol phosphates (19,76). These findings
65 were successfully translated to mammalian disease models (7,19,60). *Dictyostelium* was also
66 used to identify targets for compounds involved in bitter tastant detection (50,73) and conserved
67 roles of homologues of human proteins (38,50), to investigate mitochondrial disease (25),
68 Huntington's disease (75) and centrosomal organisation and function (29,66). These studies
69 suggest that *Dictyostelium* can inform our understanding of cellular function relevant to human
70 disease.

71 *Dictyostelium* has previously been employed to investigate the role of Ino1 in cell function (24),
72 where insertional mutagenesis of *ino1* produced an inositol auxotrophic phenotype with a
73 concomitant decrease in inositol trisphosphate. Here, we independently deleted a key region of
74 the *ino1* gene in an isogenic cell line, and find that growth of the *ino1* mutant can only be
75 partially rescued by exogenous inositol, suggesting a non-biosynthetic role for the protein. We
76 further show that the previously described ‘inositol-less death’ is likely to lead to an
77 upregulation of autophagy, loss of substrate adhesion and reduced cytokinesis resulting from
78 inositol depletion. We also show that inositol depletion leads to a generalised reduction of
79 phosphoinositide levels, without gross changes in metabolic profile. Surprisingly, we show that
80 the greatest metabolic change is caused by loss of Ino1, and not by inositol depletion *per se*,
81 since broad metabolic changes are not rescued by exogenous inositol, suggesting distinct effects
82 of Ino1 loss and inositol depletion on cellular function. Finally, we identified a range of
83 potential Ino1 binding partners, and confirmed direct Ino1 binding to a protein with mammalian
84 homologues that serve as adaptors involved in the attachment to macromolecular complexes,
85 providing a potential link to regulating inositol-independent cellular functions.

86

87 **Materials and Methods**

88 *Materials* - Axenic medium and LowFlo medium was purchased from ForMedium Co.
89 Ltd (Hunstanton, UK). All restriction enzymes and First Strand cDNA synthesis kit were
90 purchased from Fermentas (St Leon-Rot, Germany). Trizma hydrochloride (Tris-HCl), sodium
91 chloride (NaCl), ethylenediaminetetraacetic acid (EDTA), 4',6-diamidino-2-phenylindole
92 (DAPI), cyclic adenosine monophosphate (cAMP), potassium phosphate monobasic (KH₂PO₄),
93 potassium phosphate dibasic (K₂HPO₄), *myo*-inositol, and methanol were purchased from
94 Sigma (Dorset, UK). The High Pure RNA isolation kit was purchased from Roche (Welwyn

95 Garden City, UK). Penicillin-streptomycin and blasticidin were purchased from Life
96 Technologies (Gibco, UK). The DNase free kit was purchased from Ambion (Austin, TX). The
97 anti-RFP antibody [5F8], anti-GFP [3H9] and RFP-Trap or GFP-Trap agarose beads
98 (ChromoTek) were purchased from ChromoTek GmbH (Planegg-Martinsried, Germany). The
99 anti-FLAG M2 antibody (F3165) was obtained from Sigma (Dorset, UK).

100 *Cell culture, strains and plasmids* - All *Dictyostelium* axenic strains were grown at 22 °C in
101 Axenic medium containing 100 µg/ml penicillin and 100 µg/ml streptomycin. *Dictyostelium*
102 transformants with a disrupted *ino1* gene were cultured in axenic medium with 10 µg/ml
103 blasticidin and 500 µM *myo*-inositol.

104 Knock-out constructs were created by amplifying 5' and 3' fragments within the *ino1* gene by
105 PCR from genomic DNA of *Dictyostelium discoideum* axenic 2 (AX2) strain. The 5' and 3'
106 PCR fragments were cloned into the pLPBLP expression vector (21), using BamHI-PstI and
107 NcoI-KpnI restriction sites, respectively. The knock-out cassette was transformed into wild-type
108 (AX2) cells and transformants were selected in axenic medium containing blasticidin (10
109 µg/ml). Independent clones of transformants resistant to blasticidin were screened for
110 homologous integration by PCR. Loss of gene transcription was confirmed by reverse
111 transcription PCR. For this purpose, RNA was extracted from the independent clones using the
112 High Pure RNA isolation kit according to the manufacturer's instructions. Contaminating DNA
113 was removed using the DNasefree kit, followed by cDNA synthesis using the First Strand
114 cDNA synthesis kit with 1 µg of RNA per sample. The cDNA was analysed by PCR to confirm
115 loss of gene transcription (primers: GCTGCAAATCAAAGGATCGTGCC and
116 AAGGTGTTTTGTGGTGAACCATTGATG).

117 The Ino1-RFP overexpression construct was prepared using the full-length *ino1* (gene ID:
118 DDB_G0285505) open reading frame. The gene was amplified from genomic DNA using

119 EcoRI and BamHI as flanking restriction sites (primers:
120 GAGCGAATTCATGTCAGCACAAATGTTGAATC and
121 TATGGATCCTAATCTTTGTTCTAATAACATG). The PCR products were cloned into an
122 mRFPmars expression vector (389-2) under the control of the actin15 promoter (courtesy of Dr
123 Annette Müller-Taubenberger (1,23)). Constructs were transformed into the *ino1*⁻ cell line by
124 electroporation and selected for neomycin resistance (10 µg/ml). Expression of Ino1-RFP was
125 confirmed by fluorescence microscopy and western blot analysis using anti-RFP antibodies.
126 *ino1* gene expression was confirmed using reverse transcription PCR using the same method as
127 described for generating an *ino1* knock-out cell line.

128 *Development assays and cell image acquisition* - Filter assays were used to develop
129 *Dictyostelium* cells as described previously (76). Briefly, cells grown in the presence or absence
130 (24 hours) of inositol (500 µM) were harvested in log-phase growth, and 1×10^7 cells/ml were
131 plated on a 47 mm nitrocellulose filter (Millipore, Watford, UK). Filters were incubated for 24
132 hours at 22°C prior to imaging.

133 *Substrate adhesion assay* - *ino1*⁻ or Ino1-RFP-expressing *ino1*⁻ cells grown in HL5 media in the
134 presence of inositol (500 µM) were plated into 6-well plates, and the medium was replaced with
135 HL5 media in the absence or presence of inositol (500 µM). After 24 hours the medium was
136 gently removed with an aspirator to dispose of the non-adherent cells. Fresh medium was added
137 and cells were immediately re-suspended and counted, and the processes was repeated for later
138 time-points.

139 *Chemotaxis, Autophagy, and Cytokinesis assays* - Chemotaxis assays were carried out using a
140 Dunn chamber (Hawksley, Sussex, UK) as previously described (49). Images were recorded
141 every 15 seconds over a 15 min period. Autophagy was measured in *ino1*⁻ cells transformed
142 with the *atg8-GFP* construct (Dictybase.org) (46). Cells were grown in Axenic medium with

143 shaking for 72 hours (- inositol condition had inositol removed for 24 hours prior to the
144 experiment), with 16 hour incubation in LoFlo medium to reduce the background
145 autofluorescence. Cytokinesis defects were measured in cells cultured in shaking suspension for
146 72 hours, and inositol was removed where indicated 24 hours before the start of an assay, and
147 cells were fixed with 100% methanol at -20°C for 15 minutes, prior to labelling with 4',6-
148 diamidino-2-phenylindole (DAPI).

149 *Immunoprecipitation* - Initial co-immunoprecipitations were performed with the *ino1*⁻ cell line
150 constitutively expressing the *ino1-RFP* gene; *ino1*⁻ cells constitutively expressing the
151 *mRFPmars* gene on its own was used as a control (for 2 of 3 repeats) or wild-type (AX2) cell
152 lysate as a control. The presence of Ino1-RFP and RFP was confirmed by Western blot analysis
153 with anti-RFP antibody. The gel was stained with Coomassie blue and the protein bands
154 specific to Ino1-RFP (and absent in the RFP control) were evaluated by mass spectrometry and
155 the data was analysed using Scaffold3 software.

156 The *ino1*⁻ cell line co-transformed with *ino1-RFP* construct and *FLAG-gpmA*, *FLAG-pefB*, or
157 *FLAG-Q54IX5* was used to perform a co-immunoprecipitation with anti-RFP coated beads to
158 examine a direct interaction between Ino1 and these proteins. Ino1-GpmA and Ino1-Q54IX5
159 interactions were detected by Western blot analysis with anti-RFP and anti-FLAG antibodies.

160 The *ino1*⁻ cell line co-transformed with the *ino1-RFP* construct and either *GFP-gpmA* or *GFP-*
161 *Q54IX5* was used to perform co-immunoprecipitation with anti-GFP coated beads to confirm a
162 direct interaction between Ino1 and these proteins; *ino1*⁻ cells co-expressing *mRFPmars* and
163 either *GFP-gpmA* or *GFP-Q54IX5* was used as a control for these experiments. The Ino1-
164 Q54IX5 interaction was confirmed by western blot analysis with anti-GFP and anti-RFP
165 antibodies.

166 Cells (3×10^8 per experiment) were washed with phosphate buffer, treated with 2.5 mM
167 caffeine for 20 min with shaking, and lysed (0.5% NP40, 40 mM Tris-HCl, 20 mM NaCl, 5 mM
168 EGTA, 5 mM EDTA, 10 mM DTT, 1 mM PMSF, 2x protease and 2x phosphatase cocktail
169 inhibitor (Roche – cat no. 11836170001 and 04906837001)) on ice and the lysate was incubated
170 with RFP-Trap or GFP-Trap agarose beads as per manufacturer's instructions. Briefly, the
171 lysate was incubated with the beads for 1 hour at 4°C, then collected and washed twice (10 mM
172 Tris-HCl, 150 mM NaCl, 0.5 mM EDTA, 1 mM PMSF, 2x protease and 2x phosphatase
173 cocktail inhibitor). The non-bound fraction was collected after this step. Immunocomplexes
174 were dissociated from the beads by incubating at 70°C for 10 min in 4x TruPAGE LDS Sample
175 Buffer (Sigma, PCG3009) and collected by centrifugation (the bound fraction) prior to the SDS-
176 PAGE electrophoresis using either Sigma TruPAGE or BioRad pre-cast gel system. Protein
177 presence was detected with anti-GFP or anti-RFP antibodies, or a monoclonal anti-FLAG M2
178 antibody, and recorded using the Odyssey Sa infrared imaging system.

179 *NMR Spectrometry* - Freeze-dried cell pellets were resuspended in 1 mL of Water/Methanol
180 (1:2) and vortexed for polar metabolite extraction. Samples were then centrifuged at 2,400 g for
181 5 min and supernatants were kept for drying using a vacuum concentrator for 4.5 h at 45 °C.
182 Once dried, samples were resuspended in 80 μ L of phosphate buffer (in 90 % D₂O and 0.05 %
183 sodium 3-(tri-methylsilyl) propionate-2,2,3,3-d₄ (TSP) as a ¹H NMR reference) and 50 μ L of
184 the solution was transferred into 1.7 mm capillary NMR tubes. Spectra were acquired at
185 300°K on a Bruker Avance DRX 700 MHz NMR Spectrometer (Bruker Biopsin, Rheinstetten,
186 Germany) operating at 700.19 MHz and equipped with a CryoProbe™ from the same
187 manufacturer. All spectra were acquired using a 1-dimensional noesy pulse sequence [recycle
188 delay – 90° - t₁ – 90° - t_m – 90° - acquire free induction decay (FID)] with water suppression
189 applied during RD of 2 s, a mixing time (t_m) of 100 ms and a 90° pulse set at 7.70 μ s. For each
190 spectrum, 512 scans were accumulated over a spectral width of 9803.9 Hz, and all FIDs were

191 multiplied by a broadening line function of 0.3 Hz prior to Fourier transformation. All spectra
192 were manually phased, baseline-corrected and calibrated to the TSP standard at δ 0.000 using
193 the software MestReNova© (version 10.0.1, Mestrelab Research S.L., Spain).

194 *Phospholipid Analysis* - Glycerophospholipid levels were analysed by mass spectroscopy as
195 previously described (9).

196 RESULTS

197 *Ino1 protein is conserved from Dictyostelium to humans* - To investigate the role of the
198 *Dictyostelium* Ino1 protein, we first compared the *Dictyostelium* (Q54N49) and human
199 (Q9NPH2-1) protein sequences (Fig 1B,C). The proteins share 59% sequence identity
200 throughout their length, are of similar size and show common conserved NAD-binding and
201 catalytic domains (Fig 1B) that are present in Ino1 proteins from species across distant
202 biological kingdoms (Fig 1C), suggesting a highly conserved catalytic role of Ino1 throughout
203 evolution and supporting the use of *Dictyostelium* to analyze Ino1 function.

204 *ino1⁻ is an inositol auxotroph* - To analyse the effect of Ino1 loss and inositol depletion on
205 *Dictyostelium* cell growth and development, we ablated 19% of the *ino1* coding sequence,
206 including two regions encoding highly conserved amino acid motifs, by homologous integration
207 of a knockout cassette (Fig 1B-F). The resultant *ino1⁻* cells were unable to grow in liquid
208 medium without inositol supplementation above 50 μ M (Fig 2A), consistent with that shown
209 previously (24). However, unlike this previous study, inositol supplementation did not fully
210 restore the *ino1⁻* growth rate to that of the wild-type, reaching a maximal level of growth at 300
211 μ M with higher concentrations not increasing growth.

212 In *Dictyostelium*, starvation triggers cell differentiation and morphogenesis to form spore-
213 bearing fruiting bodies. We thus investigated the effect of Ino1 loss, with and without inositol
214 supplementation, on multicellular development. Wild-type and *ino1⁻* cells were starved on

215 nitrocellulose filters for 24 hours, and fruiting body morphology was recorded (Fig 2B). *inoI*
216 cells grown in the absence of inositol for 24 hours prior to nutrient deprivation were able to
217 aggregate but formed aberrant fruiting bodies (Fig 2B), a phenotype not observed for *inoI* cells
218 in an earlier report (24); however, inositol supplementation (500 μM) prior to the assay enabled
219 *inoI* cells to produce mature fruiting bodies with wild-type morphology.

220 Both growth and development phenotypes were due to lack of the Ino1 protein. This was shown
221 by expression of Ino1 linked to a C-terminal red fluorescent protein (RFP) tag in *inoI* cells,
222 which was localised in the cytosol and restored wild-type growth and development (Fig 2
223 D,E,F,G). Interestingly, since exogenous inositol did not fully restore the wild-type growth rate
224 in *inoI* cells, but Ino1-RFP did, it is likely that cells require the Ino1 protein for normal growth.
225 *inoI* cells were also unable to grow on a bacterial lawn (Fig 2G), as reported previously (29),
226 even with inositol supplementation. These results confirm a vital role of inositol in
227 *Dictyostelium* growth and development, consistent with that shown in a variety of organisms
228 throughout the kingdoms of life (40).

229 *Ino1 loss triggers inositol depletion* - We then quantified inositol levels by NMR in the *inoI*
230 and wild-type cells in the presence or absence of added inositol (Fig 3A). Wild-type cells grown
231 in un-supplemented medium contained $1.5 \pm 0.1 \mu\text{M}$ inositol, and this significantly increased to
232 $3.4 \pm 0.1 \mu\text{M}$ following inositol supplementation ($p < 0.0001$), and returned to baseline
233 following removal of inositol (Fig 3A). In contrast, *inoI* cells grown with inositol
234 supplementation had an intermediate level of inositol ($1.8 \pm 0.1 \mu\text{M}$) that significantly
235 decreased to $0.8 \pm 0.1 \mu\text{M}$ following removal of exogenous inositol for 12 hours ($p = 0.0013$).
236 A reduced level was maintained following 24 hour starvation ($1.2 \pm 0.1 \mu\text{M}$), and returned to
237 $2.0 \pm 0.1 \mu\text{M}$ following re-introduction of inositol (Fig 3B). These data confirm that in *inoI*
238 cells, inositol was depleted following withdrawal of exogenous inositol, and this trend is
239 consistent with that reported earlier (24). In addition, this data suggests that the *inoI* mutant

240 supplemented with inositol has similar intracellular inositol levels to wild-type cells (without
241 supplementation), and that differences between these cell types are likely to arise from an
242 absence of the enzyme, enabling a range of experiments to provide new insights into the distinct
243 cell and metabolic changes caused by inositol depletion and loss of Ino1.

244 *Ino1 loss causes a pleiotropic phenotype* - We first investigated potential changes in cell
245 movement during chemotaxis toward cAMP (Fig 3B). In these experiments, wild-type cells
246 showed a velocity of $9.6 \pm 1.5 \mu\text{m}/\text{min}$, with an elongated shape (aspect), and tendency for
247 single directional movement (directness) of 0.87 ± 0.14 . Loss of Ino1, with inositol
248 supplementation, caused a significant loss of elongated shape, suggesting an Ino1-dependent
249 change. In contrast, inositol depletion in *ino1* cells significantly reduced cell speed, whilst the
250 loss of shape that was also observed for Ino1 deletion was retained, and triggered increased
251 persistence. These data suggest distinct effects specific to Ino1 loss (related to loss of cell
252 shape) and to inositol depletion (loss of velocity).

253 We then examined the mechanism leading to the block in cell growth caused by loss of Ino1 in
254 the absence of exogenous inositol, previously termed “inositol-less death” (56). Since
255 autophagy can lead to cell death in response to cell stress or nutrient depletion (34), we tested
256 whether inositol depletion triggered an autophagic response. In *Dictyostelium*, formation of
257 autophagosomes can be visualised by the incorporation of a fluorescently-tagged autophagy-
258 related protein 8 (Atg8) into autophagosomal membranes (46). The *ino1* strain, grown in the
259 absence of inositol for 24 hours, showed a four-fold increase in autophagosome number per cell
260 compared to the wild-type strain (Fig 3C,D). These data suggest that inositol depletion triggered
261 an autophagic response in *ino1* cells.

262 We also examined the effect of Ino1 loss and inositol depletion on substrate attachment and
263 cytokinesis. To assess changes in cell adhesion, the number of cells attached to plates was

264 quantified up to 72 hours after the removal of exogenous inositol from the *ino1*⁻ mutant. In the
265 presence of inositol (500 μ M), *ino1*⁻ cells proliferated up to 24 hours and remained adherent
266 (Fig 3E). Upon removal of exogenous inositol, *ino1*⁻ cell number decreased to 88.5% of
267 inositol-supplemented cells after 24 hours, and to 33.5% after 72 hours. *ino1*⁻ cells expressing
268 *ino1-RFP* did not lose adhesion in the absence of exogenous inositol. We then assessed
269 cytokinesis by comparing the number of nuclei per cell in the *ino1*⁻ and wild-type strains, in the
270 presence of inositol or following inositol depletion, using a DAPI nuclear stain (Fig 3F,G) (47).
271 In these experiments, *ino1*⁻ cells showed a significant ($p < 0.001$) increase in nuclei number
272 following inositol depletion compared to the wild-type strain. Under inositol depletion
273 conditions, 24.7% of the *ino1*⁻ cells accumulated ≥ 3 nuclei compared to 7.7% of the wild-type
274 cells. This effect was rescued by growing *ino1*⁻ cells in the presence of inositol (500 μ M) (9.7%
275 of cells accumulated ≥ 3 nuclei) or by overexpressing *ino1-RFP* (Fig 3F,G) (10% of cells
276 accumulated ≥ 3 nuclei). These data suggest that inositol depletion leads to an increase in
277 autophagy, a loss of cell-substrate adhesion and a reduction in cytokinesis, but loss of *Ino1* *per*
278 *se* did not trigger these responses.

279 *Inositol depletion regulates phospholipid levels* - Since inositol is a precursor to a family of
280 inositol phospholipids (Fig 4A, B), we examined changes in phospholipid levels due to both the
281 loss of *Ino1* and as a result of inositol depletion. In *Dictyostelium*, two types of phospholipids
282 are present, diacyl phospholipids containing two acyl linkages to the glycerol backbone, and the
283 recently reported ether/acyl phospholipids containing a glycerol backbone linked to a fatty
284 alcohol at position 1 (9) (Fig 4A). We quantified the levels of both phospholipid species in
285 wild-type and *ino1*⁻ cells grown in the presence and absence of inositol (Fig 4C-Q). Separation
286 of distinct phospholipid species was limited to those of different molecular weights. We first
287 examined levels of the phospholipid precursor phosphatidic acid (PA), which comprises a
288 glycerol backbone and two fatty acid tails. Both diacyl-linked and ether-linked PA levels

289 decreased during early inositol depletion in *ino1⁻* cells (Fig 4C,D). Phosphatidylinositol (PI),
290 which is formed by the addition of the inositol head group to PA, decreased following inositol
291 depletion (in *ino1⁻*), with the greatest reduction seen in diacyl-linked PI (Fig 4E,F). A similar
292 effect was seen for the diacyl phosphatidylinositol monophosphate (PIP) (Fig 4G,H).
293 Surprisingly, inositol depletion induced a reduction in diacyl phosphatidylinositol bisphosphate
294 (PIP2) but not in ether/acyl PIP2 (Fig 4I,J). For phosphatidylinositol trisphosphate (PIP3), only
295 ether/acyl PIP3 was detectable in *ino1⁻* cells, and was reduced compared to wild-type cells,
296 independent of exogenous inositol supply (Fig 4K). The reintroduction of inositol for 12 hours
297 after 24 hour starvation restored the levels of the majority of ether/acyl and diacyl
298 phospholipids. These data suggest that the pool of diacyl phospholipids is more sensitive to
299 inositol depletion than ether/acyl species, and that cellular ether/acyl PIP2 levels are maintained
300 during these conditions.

301 Since a reduction in inositol synthesis attenuates the production of phosphoinositides, and
302 causes a transient reduction of PA, we then monitored changes in other phospholipids during
303 inositol depletion and rescue. No change in phosphatidylserine (PS) was seen in wild-type cells
304 under any condition tested; however, diacyl phosphatidylserine levels were significantly
305 increased in the *ino1⁻* cells after 24-hour inositol starvation followed by inositol re-
306 supplementation (Fig 4L,M). Phosphatidylcholine levels did not change significantly in wild-
307 type or *ino1⁻* cells under any condition (Fig 4P,Q), while the ether/acyl
308 phosphatidylethanolamine level was decreased in *ino1⁻* cells under 12-hour inositol starvation
309 (Fig 4O).

310 *Ino1 loss causes a shift to catabolic metabolism* - We next investigated the metabolic
311 consequences of both the loss of *Ino1* and inositol depletion using wild-type and *ino1⁻* cells
312 grown in the presence and absence of inositol (Fig 5). Both ablation of *ino1* and inositol
313 treatment induced specific metabolic changes. Principal component (PC) analysis of metabolic

314 profiles suggested that the greatest metabolic change was observed between the wild-type and
315 *ino1⁻* cells independent of exogenous inositol provision (Fig 5A,B), where *ino1* ablation
316 accounted for 53% of the total variance as observed in PC1. The mutation resulted in an
317 increase in amino acids and compounds related to amino acid breakdown (alanine, aspartate,
318 isoleucine, lysine, methionine, GABA, putrescine), in energy-related metabolites (fumarate,
319 lactate), in adenosine phosphorylated derivatives (5'-AMP, 3'-AMP, ATP, cAMP) and in sn-
320 glycerol-3-phosphocholine (GPC), a potent osmolyte (Fig 5B). In contrast, inositol treatment
321 accounted for only 12% of the variance between the metabolic profiles of wild-type and *ino1⁻*
322 cells as observed in PC2 (Fig 5A,C). In *ino1⁻* cells, inositol treatment resulted in increased
323 amino acid levels (leucine, methionine, tyrosine). These data suggest a dominant role for the
324 presence of the Ino1 protein (rather than inositol levels) in metabolic regulation (Fig 5).

325 Ino1 absence caused a major shift in metabolic profile, and we therefore specifically examined
326 changes caused by Ino1 loss (Fig 6A,B). This analysis showed changes in many of the
327 metabolic products found in the initial PC analysis. In contrast to a loss of Ino1, inositol
328 depletion caused limited changes to metabolic profiles. Here we specifically compared *ino1⁻*
329 cells grown in the presence or absence of inositol (12 and 24h treatments were combined since
330 they resulted in similar metabolic changes and inositol levels) (Fig 6C,D) to show that inositol
331 supplementation led to an increase of inositol and lipids, consistent with the phosphoinositide
332 analysis (Fig 4). Interestingly, reintroduction of inositol for 12 hours after 24 hour inositol
333 depletion changed the metabolic profile of *ino1⁻* cells (Fig 6E,F).

334 Supervised analysis was then used to specifically evaluate the impact of Ino1 loss on cell
335 metabolism (Fig 7). This approach suggested that Ino1 loss was associated with a significant
336 increase in some amino acids (alanine, aspartate, glycine, GABA, isoleucine, lysine,
337 methionine), and in metabolites associated with regulation of the cell cycle and DNA

338 metabolism (guanosine, ATP, deoxy-ADP, 5'AMP, 3'AMP, UTP, and β -alanine, a biomarker
339 of the degradation of pyrimidines (17)). Putrescine was also significantly increased, consistent
340 with a reduction in cell proliferation, as previously demonstrated in *Dictyostelium* (35). An
341 increase in lactate was also observed, which suggests an increase in the $\text{NADH+H}^+/\text{NAD}^+$ ratio
342 that stimulates the activity of the lactate dehydrogenase. An increase in $\text{NADH+H}^+/\text{NAD}^+$ ratio
343 would simultaneously inhibit the citrate synthase and slow down the Krebs cycle, resulting in an
344 accumulation of some intermediates. This is consistent with the accumulation of acetate,
345 derived from the spontaneous hydrolysis of oxaloacetate, and of fumarate and succinate, two
346 other intermediates of the Krebs cycle. Finally, sn-glycero-3-phosphocholine (GPC) was greatly
347 increased, suggesting that the lack of Ino1 was compensated by the production of a strong
348 osmolyte. The increased $\text{NADH+H}^+/\text{NAD}^+$ ratio is a signature of catabolic reactions. Together,
349 these data suggest that the loss of Ino1 shifts cells into a catabolic state, and further support the
350 autophagic phenotype of *ino1* mutants, even when supplemented with inositol.

351 Supervised analysis was also used to evaluate the impact of inositol depletion on individual
352 metabolites (Fig 7). This approach suggested that inositol depletion resulted in changes in some
353 amino acids (increases in alanine, GABA, glycine, and valine, and a decrease in phenylalanine),
354 an increase in lactate, fumarate, and succinate, and a decrease in 3'AMP, guanosine, and
355 glycogen. No effect on the metabolic profile was shown due to the selection antibiotic
356 (blasticidin) for the *ino1* cells (O-PLS model parameters: $R^2Y = 0.18$ and $Q^2Y = 0$). Although
357 we observed that the mutants were already in a catabolic state, the addition of inositol tended to
358 moderate this metabolic phenotype, since indicators of anabolism (glycogen and lipids) were
359 higher in cells supplemented with inositol, while those not supplemented were associated with
360 markers of catabolism (i.e. lactate and succinate). However, the absence of Ino1, rather than
361 inositol depletion, triggered broader metabolic changes.

362 *Mutation of an Ino1 catalytic residue reduces growth, independent of exogenous inositol* - To
363 investigate a role for Ino1 that is independent of catalytic activity, we expressed a mutated Ino1
364 lacking a key catalytic aspartic acid (D342A) that is conserved throughout the tree of life (40).
365 Wild-type cells expressing this construct showed strongly reduced growth, either in the
366 presence or absence of inositol (500 μ M; Fig 8A), suggesting a dominant negative effect of the
367 protein. *ino1*⁻ cells expressing this construct retained the inositol auxotrophic phenotype,
368 confirming a lack of catalytic activity of the mutated protein, but additionally showed strongly
369 reduced growth in the presence of inositol (500 μ M).

370 *Ino1 binds a possible macromolecular complex linker protein* - To investigate a mechanism for
371 Ino1 in regulating cell function independent of catalytic activity, Ino1 binding partners were
372 isolated by co-immunoprecipitation. Ino1-RFP was expressed in *ino1*⁻ cells, bound to anti-RFP
373 antibody-coated agarose beads, and were purified by co-immunoprecipitation, followed by
374 SDS-PAGE separation and mass spectrometry analysis (Fig 8B). This approach identified 104
375 potential binding partners from three independent experiments, that were divided into six major
376 groups: actin-related, immunity and stress, metabolism, nucleic acid related (translation,
377 transcription, regulation of gene expression and DNA recombination), protein catabolism,
378 modification and transport, and others encompassing signal transduction, ATP hydrolysis and
379 proton transport (including V-type proton ATPase catalytic subunits A and B) (Supplementary
380 data). We extended our analysis for three potential Ino1 binding proteins: GpmA, a
381 phosphoglycerate mutase protein that catalyses the production of 2,3-bisphospho-D-glycerate
382 (2,3BPG), which was found to accumulate in *ino1*⁻ cells starved of inositol (24); PefB, a penta-
383 EF hand domain-containing protein, linked to neurodegenerative and lysosomal diseases
384 (71,72); and Q54IX5, an uncharacterised protein with three Sell-like repeats, which was present
385 in all three independent immunoprecipitation experiments (Fig 8C,D). These proteins tagged
386 with a FLAG epitope were co-expressed in cells with Ino1-RFP, and Ino1-RFP was

387 immunoprecipitated from cell lysates with RFP antibody linked to agarose beads. The bound
388 protein fractions were then analysed for the presence of each FLAG-tagged protein,
389 demonstrating that GpmA-FLAG bound weakly, whereas Q54IX5-FLAG bound strongly to
390 Ino1-RFP (Fig 8C). The Q54IX5-Ino1 interaction was confirmed using the reverse approach,
391 where Q54IX5-GFP was coexpressed with Ino1-RFP, and immunoprecipitated with a GFP
392 antibody linked to agarose beads; co-immunoprecipitated Ino1-RFP was detected by Western
393 blot with an RFP antibody (Fig 8D). These approaches confirmed that Q54IX5 binds strongly to
394 Ino1.

395 **DISCUSSION**

396 Inositol and inositol-containing compounds are vital cellular components, and a range of studies
397 have identified pleiotropic effects of inositol depletion on cell function, but have not considered
398 complications due to altered levels of the biosynthetic enzyme, Ino1. To distinguish between the
399 effects of inositol depletion and a loss of Ino1 on cell function and metabolism, we ablated the
400 inositol biosynthetic enzyme, Ino1, in *Dictyostelium*, and compared wild-type cells and cells
401 without Ino1 in the presence and absence of inositol. Loss of Ino1 produced an inositol
402 auxotroph phenotype during growth and blocked development, confirming an earlier
403 *Dictyostelium* study (24), and results from diverse organisms ranging from *Saccharomyces*
404 *cerevisiae* (13) to mice (45), demonstrating the essential conserved role of inositol in cellular
405 function. We show that the *myo*-inositol levels decreased in the *ino1* mutant by 36-56%
406 (depending upon starvation time), and return to pre-depletion levels following inositol
407 replenishment. This inositol depletion response is consistent with an obligate role for inositol
408 production catalysed by Ino1. We show that inositol depletion resulting from *ino1* ablation
409 blocks development, reduces cell velocity, upregulates autophagy, and inhibits cytokinesis,
410 consistent with a range of studies in other systems (12, 24, 37, 51, 62), and confirming the
411 validity of this model to study Ino1 function. All of these phenotypes, except growth and cell

412 shape, are rescued by provision of exogenous inositol, and are thus likely to be due to inositol
413 depletion rather than loss of Ino1.

414 Dysregulation of inositol levels has been reported in a wide range of biomedical and clinical
415 studies, relating to both disease conditions and as a result of medicinal treatment, although few
416 studies have addressed specific changes in Ino1 protein levels. A range of structurally
417 independent bipolar disorder drugs, including carbamazepine, valproate and lithium, act via an
418 inositol depletion mechanism (76), and induce autophagy *in vitro* and *in vivo* (43,67), to
419 promote survival by recycling cellular components (12,51). Altered inositol levels have also
420 been demonstrated in patient studies of bipolar disorder (58), major depressive disorder (10),
421 and schizophrenia (59). For these reasons, modulating inositol levels was proposed as a therapy
422 in the treatment of bipolar disorder (8), depression, and panic disorders (48). In addition, Ino1
423 activity and protein levels are elevated in post-mortem brains of Alzheimer's patients (57),
424 although studies showed pathologically-lowered inositol levels and mitochondrial dysfunction
425 in mouse models of Alzheimer's disease (68) that could be linked to autophagy (36). However,
426 no distinction has been made in these studies between altered inositol levels and altered Ino1
427 levels. In our present study, we have separated the effects caused by altered Ino1 levels and
428 inositol depletion, to provide a unique approach to monitor cellular and metabolic changes
429 relating to inositol levels.

430 Since phosphoinositide production is the first step of inositol incorporation into cell signalling,
431 we examined the effect of loss of Ino1 and inositol depletion on this family of chemicals,
432 analysing both diacyl-linked and ether/acyl-linked compounds independently (9). Inositol
433 depletion induced a rapid reduction in both species of PI and PIP, and strongly reduced diacyl
434 PIP2 levels, but had little effect on ether/acyl PIP2. Surprisingly, PIP3 was greatly reduced in
435 the *ino1*⁻ mutant, under all conditions, independent of exogenous inositol. Overall, the greater
436 reduction in diacyl-phosphoinositides, comprising under 5% of the inositol phospholipids (9),

437 may be due to the preferential metabolism of these species above that of the ether/acyl
438 derivatives as precursors of inositol phosphates. Alternatively, these compounds may provide a
439 more labile signalling component, giving rise to more rapid metabolism compared to ether-
440 derived compounds, and further research could investigate these alternatives. Nevertheless, this
441 data shows a critical effect of inositol depletion in regulating phosphoinositides.

442 These results also support an important role for diacyl PIP2 in vesicle formation and transport
443 (32) and in membrane trafficking at the neuronal synapse (11). In *Dictyostelium*, ablation of a
444 PIP2 biosynthetic enzyme PIP5 kinase (PikI) led to a 90% reduction in PIP2 levels, and
445 disorientated cell movement (22). The pivotal role of PIP2 in these processes suggests a
446 requirement for cells to maintain the levels of this essential molecule during inositol starvation.
447 Cytokinesis is also critically dependent upon an increase in PIP2 levels (37), and a 65%
448 reduction in diacyl PIP2 levels following 24-hour inositol depletion is consistent with a block in
449 cytokinesis giving rise to the multinucleate phenotype of *inoI*⁻ cells. In a similar manner, PIP2
450 is involved in substrate attachment by regulating actin polymerisation and depolymerisation
451 (37) that may result in a reduced cell-substrate adhesion. Overall, the data suggest that inositol
452 depletion has a fundamental and rapid effect on phosphoinositide regulation that is likely to
453 result in wide-ranging changes in cellular function and cell health.

454 Interestingly, Ino1 may play a role in regulating PIP3 levels regardless of inositol level, since
455 the *inoI*⁻ mutant grown in inositol-supplemented medium showed reduced PIP3 levels, even
456 though intracellular *myo*-inositol levels were comparable to those of wild-type cells. Previous
457 studies in *Dictyostelium* demonstrated that a complete block in PIP3 production, by deletion of
458 all five phosphoinositide 3-kinase enzymes, resulted in poor growth and developmental defects
459 (27). Combined, these findings suggest that loss of the Ino1 protein leads to a loss of PIP3
460 production, resulting in poor cell growth.

461 We also examined metabolic changes caused by loss of the Ino1 protein and during inositol
462 depletion. Surprisingly, the greatest metabolic change observed here was due to an absence of
463 Ino1 which gave rise to elevated amino acids, energy-related components, DNA regulation and
464 osmolytes. This metabolic shift was not due to altered inositol levels *per se*, since cellular
465 inositol levels are consistent between the mutant and wild-type cells during inositol
466 supplementation, but rather an absence of the Ino1 protein. These changes are likely to have a
467 major effect on cellular function, and suggest an important non-catalytic role for the protein in
468 metabolic regulation, shifting metabolism towards an autophagic response, with increased
469 levels of putrescine, amino acids and nucleotide derivatives (31). In contrast, inositol depletion
470 caused general changes in lipids, and variable changes in a few amino acids. This suggests
471 inositol depletion has little metabolic effect in the short timescale examined in this study.

472 Since inositol supplementation did not fully restore *ino1⁻* growth, we expressed a mutant protein
473 Ino1-D342A in these cells and assessed growth. This mutation is likely to disrupt catalytic
474 activity and is conserved in all known Ino1 proteins. Expression of Ino1-D342A did not rescue
475 the inositol auxotrophy resulting from Ino1 loss, and thus does not catalyse inositol
476 biosynthesis. In contrast, expression of the protein reduced growth in all strains, independently
477 of exogenous inositol provision. Further studies will be necessary to determine if this response
478 is due to the depletion of the Ino1 substrate, inactivation of a potential Ino1 multimeric
479 complex, or by other mechanisms.

480 To identify new roles for Ino1 in regulation of cellular function, we isolated a number of
481 potential Ino1 binding partners. These included proteins related to cytoskeletal organisation,
482 mitochondrial function, DNA and protein regulation, and metabolism, including fatty acid,
483 glycolysis and purine metabolism and vacuolar ATPase; consistent with those identified in *S.*
484 *cerevisiae* (16,63,64) and in humans (20). From the list of potential binding partners, we
485 independently confirmed Ino1-GpmA binding, where GpmA catalyses the production of 2,3-

486 bisphosphoglycerate (2,3BPG) from 2- or 3-phosphoglycerate. Importantly, 2,3 BPG potently
487 inhibits the dephosphorylation of InsP_3 and InsP_2 (70), relating to the effect of lithium on the
488 dephosphorylation of IP_1 (74) and is elevated following *ino1* loss in *Dictyostelium* (24). The
489 binding of Ino1-GpmA thus provides a potentially crucial link between loss of Ino1 and a
490 mechanism of inositol depletion similar to that of lithium. We also confirmed strong Ino1-
491 Q54IX5 binding, where this protein contains a tetratricopeptide repeat (TPR) that mediates
492 protein-protein interactions, often during the assembly of multiprotein complexes (5). Although
493 the function of an Ino1-Q54IX5 interaction remains to be examined, the potential human
494 orthologue of Q54IX5 is the SEL1L protein that is involved in the movement of misfolded
495 proteins from the ER to the cytosol and in protein ubiquitination (44), and thus dysregulation of
496 this protein in the *ino1*⁻ mutant may have far-reaching effect on cell function.

497 Since we show that the absence of Ino1 and inositol depletion have different molecular and
498 metabolic effects, we question whether these effects are interrelated. Inositol depletion has been
499 shown to activate *ino1* expression in a wide range of models (55,69), including *Dictyostelium*
500 (76), and mice (54); this effect is likely to elevate Ino1 levels. Many studies have relied on
501 using inositol depleting drugs prescribed as bipolar disorder treatments, which act through
502 multiple targets (28,53,65,77), and hence these studies are likely to be complicated by
503 secondary effects. In contrast, our study did not utilise drug treatments, and suggest that short-
504 term inositol depletion does not cause large metabolic changes in *Dictyostelium*, enabling a
505 subsequent increase in *ino1* transcription acting to reverse this deficit (76). This responsive
506 regulation would protect cells against a transient reduction in inositol levels without triggering
507 large metabolic changes, with a dysregulation of this responsive mode resulting from a
508 reduction of Ino1 levels, causing wide-ranging metabolic effects.

509 To sum up, our studies show that a loss of the crucial inositol biosynthetic enzyme Ino1 and
510 inositol depletion cause discrete cellular, molecular and metabolic effects. Although inositol

511 depletion alters cell physiology, triggering an autophagic response, loss of substrate adhesion,
512 reduction in cell division, and a rapid reduction in a range of phospholipids, it does not trigger a
513 large change in metabolic profile. In contrast, the Ino1 protein itself plays an important role in
514 cell growth and shape and metabolic regulation, regardless of inositol level, including the
515 binding to a linker protein, Q54IX5, suggesting further roles of this protein.

516

517 **Acknowledgments**

518 None

519 **Funding information**

520 This work was funded by a grant to RSBW by The Dr Hadwen Trust for Humane Research
521 (DHT), which is the UK leading medical research charity that funds and promotes
522 exclusively human-relevant research that encourages the progress of medicine with the
523 replacement of the use of animals in research. GO was supported by NC3Rs Grant
524 NC/M001504/1.

525 **Conflict of interests**

526 None.

527 **Author Contributions**

528 RSBW and AF planned the experiments. AF, JC, CLR, GPO, GC, SPC, PH, LS, SL, PT, RI
529 carried out all experimental procedures and data analysis. RSBW and AF wrote the paper.

530 **Supplementary data will be available at the following site: DOIxxxxx**

531

532

Reference List

533

534 1. **Basu, S., P. Fey, Y. Pandit, R. Dodson, W. A. Kibbe, and R. L. Chisholm.** 2013. DictyBase 2013:
535 integrating multiple Dictyostelid species. *Nucleic Acids Res.* **41**:D676-D683. doi:gks1064
536 [pii];10.1093/nar/gks1064 [doi].

537 2. **Berridge, M. J.** 2014. Calcium regulation of neural rhythms, memory and Alzheimer's disease.
538 *J.Physiol* **592**:281-293. doi:jphysiol.2013.257527 [pii];10.1113/jphysiol.2013.257527 [doi].

539 3. **Berridge, M. J.** 2014. Calcium signalling and psychiatric disease: bipolar disorder and
540 schizophrenia. *Cell Tissue Res.* **357**:477-492. doi:10.1007/s00441-014-1806-z [doi].

541 4. **Berridge, M. J., C. P. Downes, and M. R. Hanley.** 1989. Neural and developmental actions of
542 lithium: a unifying hypothesis. *Cell* **59**:411-419.

543 5. **Blatch, G. L. and M. Lassle.** 1999. The tetratricopeptide repeat: a structural motif mediating
544 protein-protein interactions. *Bioessays* **21**:932-939. doi:10.1002/(SICI)1521-
545 1878(199911)21:11<932::AID-BIES5>3.0.CO;2-N [pii];10.1002/(SICI)1521-
546 1878(199911)21:11<932::AID-BIES5>3.0.CO;2-N [doi].

547 6. **Chang, P., B. Orabi, R. M. Deranieh, M. Dham, O. Hoeller, J. A. Shimshoni, B. Yagen, M.**
548 **Bialer, M. L. Greenberg, M. C. Walker, and R. S. Williams.** 2012. The antiepileptic drug
549 valproic acid and other medium-chain fatty acids acutely reduce phosphoinositide levels
550 independently of inositol in Dictyostelium. *Dis.Model.Mech.* **5**:115-124. doi:dmm.008029
551 [pii];10.1242/dmm.008029 [doi].

552 7. **Chang, P., M. C. Walker, and R. S. Williams.** 2014. Seizure-induced reduction in PIP3 levels
553 contributes to seizure-activity and is rescued by valproic acid. *Neurobiol.Dis.* **62**:296-306.
554 doi:S0969-9961(13)00292-1 [pii];10.1016/j.nbd.2013.10.017 [doi].

555 8. **Chengappa, K. N., J. Levine, S. Gershon, A. G. Mallinger, A. Hardan, A. Vagnucci, B. Pollock, J.**
556 **Luther, J. Battenfield, S. Verfaillie, and D. J. Kupfer.** 2000. Inositol as an add-on treatment for
557 bipolar depression. *Bipolar.Disord.* **2**:47-55.

558 9. **Clark, J., R. R. Kay, A. Kielkowska, I. Niewczas, L. Fets, D. Oxley, L. R. Stephens, and P. T.**
559 **Hawkins.** 2014. Dictyostelium uses ether-linked inositol phospholipids for intracellular
560 signalling. *EMBO J.* **33**:2188-2200. doi:embj.201488677 [pii];10.15252/embj.201488677 [doi].

561 10. **Coupland, N. J., C. J. Ogilvie, K. M. Hegadoren, P. Seres, C. C. Hanstock, and P. S. Allen.** 2005.
562 Decreased prefrontal Myo-inositol in major depressive disorder. *Biol.Psychiatry* **57**:1526-1534.
563 doi:S0006-3223(05)00233-7 [pii];10.1016/j.biopsych.2005.02.027 [doi].

564 11. **Cremona, O. and C. P. De.** 2001. Phosphoinositides in membrane traffic at the synapse. *J.Cell*
565 *Sci.* **114**:1041-1052.

566 12. **Criollo, A., M. C. Maiuri, E. Tasdemir, I. Vitale, A. A. Fiebig, D. Andrews, J. Molgo, J. Diaz, S.**
567 **Lavandro, F. Harper, G. Pierron, S. D. di, R. Rizzuto, G. Szabadkai, and G. Kroemer.** 2007.
568 Regulation of autophagy by the inositol trisphosphate receptor. *Cell Death.Differ.* **14**:1029-
569 1039. doi:4402099 [pii];10.1038/sj.cdd.4402099 [doi].

570 13. **Culbertson, M. R., T. F. Donahue, and S. A. Henry.** 1976. Control of inositol biosynthesis in
571 *Saccharomyces cerevisiae*: properties of a repressible enzyme system in extracts of wild-type
572 (Ino+) cells. *J.Bacteriol.* **126**:232-242.

- 573 14. **De Camilli, P., S. D. Emr, P. S. McPherson, and P. Novick.** 1996. Phosphoinositides as
574 regulators in membrane traffic. *Science* **271**:1533-1539.
- 575 15. **Deraniew, R. M. and M. L. Greenberg.** 2009. Cellular consequences of inositol depletion.
576 *Biochem.Soc.Trans.* **37**:1099-1103. doi:BST0371099 [pii];10.1042/BST0371099 [doi].
- 577 16. **Deraniew, R. M., Y. Shi, M. Tarsio, Y. Chen, J. M. McCaffery, P. M. Kane, and M. L. Greenberg.**
578 2015. Perturbation of the Vacuolar ATPase: A NOVEL CONSEQUENCE OF INOSITOL DEPLETION.
579 *J.Biol.Chem* **290**:27460-27472. doi:M115.683706 [pii];10.1074/jbc.M115.683706 [doi].
- 580 17. **Di, M., I. C. Lamperti, and V. Tiranti.** 2015. Mitochondrial diseases caused by toxic compound
581 accumulation: from etiopathology to therapeutic approaches. *EMBO Mol.Med.* **7**:1257-1266.
582 doi:emmm.201505040 [pii];10.15252/emmm.201505040 [doi].
- 583 18. **Dowler, S., L. Montalvo, D. Cantrell, N. Morrice, and D. R. Alessi.** 2000. Phosphoinositide 3-
584 kinase-dependent phosphorylation of the dual adaptor for phosphotyrosine and 3-
585 phosphoinositides by the Src family of tyrosine kinase. *Biochem.J.* **349**:605-610.
- 586 19. **Eickholt, B. J., G. Towers, W. J. Ryves, D. Eikel, K. Adley, L. Ylinen, N. Chadborn, A. Harwood,
587 H. Nau, and R. S. Williams.** 2005. Effects of valproic acid derivatives on inositol trisphosphate
588 depletion, teratogenicity, GSK-3 β inhibition and viral replication - A screening approach for
589 new bipolar disorder drugs based on the valproic acid core structure. *Mol.Pharmacol.* **67**:1-8.
- 590 20. **Emdal, K. B., A. K. Pedersen, D. B. Bekker-Jensen, K. P. Tsafou, H. Horn, S. Lindner, J. H.
591 Schulte, A. Eggert, L. J. Jensen, C. Francavilla, and J. V. Olsen.** 2015. Temporal proteomics of
592 NGF-TrkA signaling identifies an inhibitory role for the E3 ligase Cbl-b in neuroblastoma cell
593 differentiation. *Sci.Signal.* **8**:ra40. doi:8/374/ra40 [pii];10.1126/scisignal.2005769 [doi].
- 594 21. **Faix, J., L. Kreppel, G. Shaulsky, M. Schleicher, and A. R. Kimmel.** 2004. A rapid and efficient
595 method to generate multiple gene disruptions in *Dictyostelium discoideum* using a single
596 selectable marker and the Cre-loxP system. *Nucleic Acids Res.* **32**:e143.
- 597 22. **Fets, L., J. M. Nichols, and R. R. Kay.** 2014. A PIP5 kinase essential for efficient chemotactic
598 signaling. *Curr.Biol.* **24**:415-421. doi:S0960-9822(13)01611-4 [pii];10.1016/j.cub.2013.12.052
599 [doi].
- 600 23. **Fey, P., R. J. Dodson, S. Basu, and R. L. Chisholm.** 2013. One stop shop for everything
601 Dictyostelium: dictyBase and the Dicty Stock Center in 2012. *Methods Mol.Biol.* **983**:59-92.
602 doi:10.1007/978-1-62703-302-2_4 [doi].
- 603 24. **Fischbach, A., S. Adelt, A. Muller, and G. Vogel.** 2006. Disruption of inositol biosynthesis
604 through targeted mutagenesis in *Dictyostelium discoideum*: generation and characterization
605 of inositol-auxotrophic mutants. *Biochem.J.* **397**:509-518. doi:BJ20060277
606 [pii];10.1042/BJ20060277 [doi].
- 607 25. **Francione, L. M. and P. R. Fisher.** 2011. Heteroplasmic mitochondrial disease in *Dictyostelium*
608 *discoideum*. *Biochem.Pharmacol.* **82**:1510-1520. doi:S0006-2952(11)00529-6
609 [pii];10.1016/j.bcp.2011.07.071 [doi].
- 610 26. **Gelber, D., J. Levine, and R. H. Belmaker.** 2001. Effect of inositol on bulimia nervosa and binge
611 eating. *Int.J.Eat.Disord.* **29**:345-348. doi:10.1002/eat.1028 [pii].

- 612 27. **Hoeller, O. and R. R. Kay.** 2007. Chemotaxis in the absence of PIP3 gradients. *Curr.Biol.*
613 **17**:813-817.
- 614 28. **Ju, S. and M. L. Greenberg.** 2003. Valproate disrupts regulation of inositol responsive genes
615 and alters regulation of phospholipid biosynthesis. *Mol.Microbiol.* **49**:1595-1603.
- 616 29. **Junemann, A., M. Winterhoff, B. Nordholz, K. Rottner, L. Eichinger, R. Graf, and J. Faix.** 2013.
617 ForC lacks canonical formin activity but bundles actin filaments and is required for
618 multicellular development of *Dictyostelium* cells. *Eur.J.Cell Biol.* **92**:201-212. doi:S0171-
619 9335(13)00046-0 [pii];10.1016/j.ejcb.2013.07.001 [doi].
- 620 30. **Kennington, A. S., C. R. Hill, J. Craig, C. Bogardus, I. Raz, H. K. Ortmeyer, B. C. Hansen, G.**
621 **Romero, and J. Larnar.** 1990. Low urinary chiro-inositol excretion in non-insulin-dependent
622 diabetes mellitus. *N.Engl.J.Med.* **323**:373-378. doi:10.1056/NEJM199008093230603 [doi].
- 623 31. **Kim, K. H. and M. S. Lee.** 2014. Autophagy—a key player in cellular and body metabolism.
624 *Nat.Rev.Endocrinol.* **10**:322-337. doi:nrendo.2014.35 [pii];10.1038/nrendo.2014.35 [doi].
- 625 32. **Klopfenstein, D. R., M. Tomishige, N. Stuurman, and R. D. Vale.** 2002. Role of
626 phosphatidylinositol(4,5)bisphosphate organization in membrane transport by the Unc104
627 kinesin motor. *Cell* **109**:347-358. doi:S0092867402007080 [pii].
- 628 33. **Kofman, O., W. R. Sherman, V. Katz, and R. H. Belmaker.** 1993. Restoration of brain myo-
629 inositol levels in rats increases latency to lithium-pilocarpine seizures. *Psychopharmacology*
630 (Berl) **110**:229-234.
- 631 34. **Kosta, A., C. Roisin-Bouffay, M. F. Luciani, G. P. Otto, R. H. Kessin, and P. Golstein.** 2004.
632 Autophagy gene disruption reveals a non-vacuolar cell death pathway in *Dictyostelium*.
633 *J.Biol.Chem* **279**:48404-48409. doi:10.1074/jbc.M408924200 [doi];M408924200 [pii].
- 634 35. **Kumar, R., S. Rafia, and S. Saran.** 2014. Cloning, expression and characterization of the
635 ornithine decarboxylase gene from *Dictyostelium discoideum*. *Int.J.Dev.Biol.* **58**:669-676.
636 doi:140174ss [pii];10.1387/ijdb.140174ss [doi].
- 637 36. **Lionaki, E., M. Markaki, K. Palikaras, and N. Tavernarakis.** 2015. Mitochondria, autophagy and
638 age-associated neurodegenerative diseases: New insights into a complex interplay.
639 *Biochim.Biophys.Acta* **1847**:1412-1423. doi:S0005-2728(15)00068-7
640 [pii];10.1016/j.bbabi.2015.04.010 [doi].
- 641 37. **Logan, M. R. and C. A. Mandato.** 2006. Regulation of the actin cytoskeleton by PIP2 in
642 cytokinesis. *Biol.Cell* **98**:377-388. doi:BC20050081 [pii];10.1042/BC20050081 [doi].
- 643 38. **Ludtmann, M. H., G. P. Otto, C. Schilde, Z. H. Chen, C. Y. Allan, S. Brace, P. W. Beesley, A. R.**
644 **Kimmel, P. Fisher, R. Killick, and R. S. Williams.** 2014. An ancestral non-proteolytic role for
645 presenilin proteins in multicellular development of the social amoeba *Dictyostelium*
646 *discoideum*. *J.Cell Sci.* **127**:1576-1584. doi:jcs.140939 [pii];10.1242/jcs.140939 [doi].
- 647 39. **Maeba, R., H. Hara, H. Ishikawa, S. Hayashi, N. Yoshimura, J. Kusano, Y. Takeoka, D. Yasuda,**
648 **T. Okazaki, M. Kinoshita, and T. Teramoto.** 2008. Myo-inositol treatment increases serum
649 plasmalogens and decreases small dense LDL, particularly in hyperlipidemic subjects with
650 metabolic syndrome. *J.Nutr.Sci.Vitaminol.(Tokyo)* **54**:196-202. doi:JST.JSTAGE/jnsv/54.196
651 [pii].

- 652 40. **Majumder, A. L., A. Chatterjee, D. K. Ghosh, and M. Majee.** 2003. Diversification and
653 evolution of L-myo-inositol 1-phosphate synthase. *FEBS Lett.* **553**:3-10.
654 doi:S0014579303009748 [pii].
- 655 41. **McLaurin, J., T. Franklin, A. Chakrabartty, and P. E. Fraser.** 1998. Phosphatidylinositol and
656 inositol involvement in Alzheimer amyloid-beta fibril growth and arrest. *J.Mol.Biol.* **278**:183-
657 194. doi:S0022-2836(98)91677-1 [pii];10.1006/jmbi.1998.1677 [doi].
- 658 42. **Michell, R. H., V. L. Heath, M. A. Lemmon, and S. K. Dove.** 2006. Phosphatidylinositol 3,5-
659 bisphosphate: metabolism and cellular functions. *Trends Biochem.Sci.* **31**:52-63. doi:S0968-
660 0004(05)00343-9 [pii];10.1016/j.tibs.2005.11.013 [doi].
- 661 43. **Motoi, Y., K. Shimada, K. Ishiguro, and N. Hattori.** 2014. Lithium and autophagy. *ACS Chem*
662 *Neurosci.* **5**:434-442. doi:10.1021/cn500056q [doi].
- 663 44. **Mueller, B., E. J. Klemm, E. Spooner, J. H. Claessen, and H. L. Ploegh.** 2008. SEL1L nucleates a
664 protein complex required for dislocation of misfolded glycoproteins. *Proc.Natl.Acad.Sci.U.S.A*
665 **105**:12325-12330. doi:0805371105 [pii];10.1073/pnas.0805371105 [doi].
- 666 45. **Ohnishi, T., T. Murata, A. Watanabe, A. Hida, H. Ohba, Y. Iwayama, K. Mishima, Y. Gondo,**
667 **and T. Yoshikawa.** 2014. Defective craniofacial development and brain function in a mouse
668 model for depletion of intracellular inositol synthesis. *J.Biol.Chem* **289**:10785-10796.
669 doi:M113.536706 [pii];10.1074/jbc.M113.536706 [doi].
- 670 46. **Otto, G. P., M. Y. Wu, N. Kazgan, O. R. Anderson, and R. H. Kessin.** 2003. Macroautophagy is
671 required for multicellular development of the social amoeba *Dictyostelium discoideum*.
672 *J.Biol.Chem* **278**:17636-17645. doi:10.1074/jbc.M212467200 [doi];M212467200 [pii].
- 673 47. **Pakes, N. K., D. M. Veltman, F. Rivero, J. Nasir, R. Insall, and R. S. Williams.** 2012. The Rac GEF
674 ZizB regulates development, cell motility and cytokinesis in *Dictyostelium*. *J.Cell Sci.* **125**:2457-
675 2465. doi:jcs.100966 [pii];10.1242/jcs.100966 [doi].
- 676 48. **Palatnik, A., K. Frolov, M. Fux, and J. Benjamin.** 2001. Double-blind, controlled, crossover trial
677 of inositol versus fluvoxamine for the treatment of panic disorder. *J.Clin.Psychopharmacol.*
678 **21**:335-339.
- 679 49. **Robery, S., J. Mukanowa, S. N. Percie du, P. L. Andrews, and R. S. Williams.** 2011.
680 Investigating the effect of emetic compounds on chemotaxis in *Dictyostelium* identifies a non-
681 sentient model for bitter and hot tastant research. *PLoS.One.* **6**:e24439.
682 doi:10.1371/journal.pone.0024439 [doi];PONE-D-11-04761 [pii].
- 683 50. **Robery, S., R. Tyson, C. Dinh, A. Kuspa, A. A. Noegel, T. Bretschneider, P. L. Andrews, and R.**
684 **S. Williams.** 2013. A novel human receptor involved in bitter tastant detection identified using
685 *Dictyostelium discoideum*. *J.Cell Sci.* **126**:5465-5476. doi:jcs.136440 [pii];10.1242/jcs.136440
686 [doi].
- 687 51. **Schiebler, M., K. Brown, K. Hegyi, S. M. Newton, M. Renna, L. Hepburn, C. Klapholz, S.**
688 **Coulter, A. Obregon-Henao, T. M. Henao, R. Basaraba, B. Kampmann, K. M. Henry, J. Burgon,**
689 **S. A. Renshaw, A. Fleming, R. R. Kay, K. E. Anderson, P. T. Hawkins, D. J. Ordway, D. C.**
690 **Rubinsztein, and R. A. Floto.** 2015. Functional drug screening reveals anticonvulsants as
691 enhancers of mTOR-independent autophagic killing of *Mycobacterium tuberculosis* through
692 inositol depletion. *EMBO Mol.Med.* **7**:127-139. doi:emmm.201404137
693 [pii];10.15252/emmm.201404137 [doi].

- 694 52. **Scioscia, M., S. Kunjara, K. Gumaa, P. McLean, C. H. Rodeck, and T. W. Rademacher.** 2007.
695 Urinary excretion of inositol phosphoglycan P-type in gestational diabetes mellitus.
696 *Diabet.Med.* **24**:1300-1304. doi:DME2267 [pii];10.1111/j.1464-5491.2007.02267.x [doi].
- 697 53. **Shaltiel, G., S. Mark, O. Kofman, R. H. Belmaker, and G. Agam.** 2007. Effect of valproate
698 derivatives on human brain myo-inositol-1-phosphate (MIP) synthase activity and
699 amphetamine-induced rearing. *Pharmacol.Rep.* **59**:402-407.
- 700 54. **Shamir, A., G. Shaltiel, M. L. Greenberg, R. H. Belmaker, and G. Agam.** 2003. The effect of
701 lithium on expression of genes for inositol biosynthetic enzymes in mouse hippocampus; a
702 comparison with the yeast model. *Brain Res.Mol.Brain Res.* **115**:104-110.
- 703 55. **Shetty, A., A. Swaminathan, and J. M. Lopes.** 2013. Transcription regulation of a yeast gene
704 from a downstream location. *J.Mol.Biol.* **425**:457-465. doi:S0022-2836(12)00890-X
705 [pii];10.1016/j.jmb.2012.11.018 [doi].
- 706 56. **Shi, Y., D. L. Vaden, S. Ju, D. Ding, J. H. Geiger, and M. L. Greenberg.** 2005. Genetic
707 perturbation of glycolysis results in inhibition of de novo inositol biosynthesis. *J.Biol.Chem*
708 **280**:41805-41810. doi:M505181200 [pii];10.1074/jbc.M505181200 [doi].
- 709 57. **Shimohama, S., H. Tanino, Y. Sumida, J. Tsuda, and S. Fujimoto.** 1998. Alteration of myo-
710 inositol monophosphatase in Alzheimer's disease brains. *Neurosci.Lett.* **245**:159-162.
711 doi:S0304394098002092 [pii].
- 712 58. **Shimon, H., G. Agam, R. H. Belmaker, T. M. Hyde, and J. E. Kleinman.** 1997. Reduced frontal
713 cortex inositol levels in postmortem brain of suicide victims and patients with bipolar disorder.
714 *Am.J.Psychiatry* **154**:1148-1150. doi:10.1176/ajp.154.8.1148 [doi].
- 715 59. **Shimon, H., Y. Sobolev, M. Davidson, V. Haroutunian, R. H. Belmaker, and G. Agam.** 1998.
716 Inositol levels are decreased in postmortem brain of schizophrenic patients. *Biol.Psychiatry*
717 **44**:428-432. doi:S0006-3223(98)00071-7 [pii].
- 718 60. **Shimshoni, J. A., E. C. Dalton, A. Jenkins, S. Eyal, K. Kwan, R. S. Williams, N. Pessah, B. Yagen,**
719 **A. J. Harwood, and M. Bialer.** 2007. The effects of CNS-active Valproic acid constitutional
720 isomers, cyclopropyl analogues and amide derivatives on neuronal growth cone behaviour.
721 *Mol.Pharmacol.* **71**:884-892.
- 722 61. **Silverstone, P. H., B. M. McGrath, and H. Kim.** 2005. Bipolar disorder and myo-inositol: a
723 review of the magnetic resonance spectroscopy findings. *Bipolar.Disord.* **7**:1-10. doi:BDI174
724 [pii];10.1111/j.1399-5618.2004.00174.x [doi].
- 725 62. **Steger, D. J., E. S. Haswell, A. L. Miller, S. R. Wentz, and E. K. O'Shea.** 2003. Regulation of
726 chromatin remodeling by inositol polyphosphates. *Science* **299**:114-116.
727 doi:10.1126/science.1078062 [doi];1078062 [pii].
- 728 63. **Szappanos, B., K. Kovacs, B. Szamecz, F. Honti, M. Costanzo, A. Baryshnikova, G. Gelius-**
729 **Dietrich, M. J. Lercher, M. Jelasity, C. L. Myers, B. J. Andrews, C. Boone, S. G. Oliver, C. Pal,**
730 **and B. Papp.** 2011. An integrated approach to characterize genetic interaction networks in
731 yeast metabolism. *Nat.Genet.* **43**:656-662. doi:ng.846 [pii];10.1038/ng.846 [doi].
- 732 64. **Tarassov, K., V. Messier, C. R. Landry, S. Radinovic, M. M. Serna Molina, I. Shames, Y.**
733 **Malitskaya, J. Vogel, H. Bussey, and S. W. Michnick.** 2008. An in vivo map of the yeast protein
734 interactome. *Science* **320**:1465-1470. doi:1153878 [pii];10.1126/science.1153878 [doi].

- 735 65. **Terbach, N. and R. S. Williams.** 2009. Structure-function studies for the panacea, valproic acid.
736 *Biochem.Soc.Trans* **37**:1126-1132.
- 737 66. **Tikhonenko, I., V. Magidson, R. Graf, A. Khodjakov, and M. P. Koonce.** 2013. A kinesin-
738 mediated mechanism that couples centrosomes to nuclei. *Cell Mol.Life Sci.* **70**:1285-1296.
739 doi:10.1007/s00018-012-1205-0 [doi].
- 740 67. **Toker, L., Y. Bersudsky, I. Plaschkes, V. Chalifa-Caspi, G. T. Berry, R. Buccafusca, D. Moechars,**
741 **R. H. Belmaker, and G. Agam.** 2014. Inositol-related gene knockouts mimic lithium's effect on
742 mitochondrial function. *Neuropsychopharmacology* **39**:319-328. doi:npp2013194
743 [pii];10.1038/npp.2013.194 [doi].
- 744 68. **Trushina, E., E. Nemutlu, S. Zhang, T. Christensen, J. Camp, J. Mesa, A. Siddiqui, Y. Tamura, H.**
745 **Sesaki, T. M. Wengenack, P. P. Dzeja, and J. F. Poduslo.** 2012. Defects in mitochondrial
746 dynamics and metabolomic signatures of evolving energetic stress in mouse models of familial
747 Alzheimer's disease. *PLoS.One.* **7**:e32737. doi:10.1371/journal.pone.0032737 [doi];PONE-D-11-
748 21642 [pii].
- 749 69. **Vaden, D. L., D. Ding, B. Peterson, and M. L. Greenberg.** 2001. Lithium and valproate decrease
750 inositol mass and increase expression of the yeast INO1 and INO2 genes for inositol
751 biosynthesis. *J.Biol.Chem.* **276**:15466-15471.
- 752 70. **Van Lookeren Campagne, M. M., C. Erneux, E. R. Van, and P. J. Van Haastert.** 1988. Two
753 dephosphorylation pathways of inositol 1,4,5-trisphosphate in homogenates of the cellular
754 slime mould *Dictyostelium discoideum*. *Biochem.J.* **254**:343-350.
- 755 71. **Vergarajauregui, S., J. A. Martina, and R. Puertollano.** 2009. Identification of the penta-EF-
756 hand protein ALG-2 as a Ca²⁺-dependent interactor of mucolipin-1. *J.Biol.Chem* **284**:36357-
757 36366. doi:M109.047241 [pii];10.1074/jbc.M109.047241 [doi].
- 758 72. **Vito, P., E. Lacana, and L. D'Adamio.** 1996. Interfering with apoptosis: Ca²⁺-binding protein
759 ALG-2 and Alzheimer's disease gene ALG-3. *Science* **271**:521-525.
- 760 73. **Waheed, A., M. H. Ludtmann, N. Pakes, S. Robery, A. Kuspa, C. Dinh, D. Baines, R. S.**
761 **Williams, and M. A. Carew.** 2014. Naringenin inhibits the growth of *Dictyostelium* and MDCK-
762 derived cysts in a TRPP2 (polycystin-2)-dependent manner. *Br.J.Pharmacol.* **171**:2659-2670.
763 doi:10.1111/bph.12443 [doi].
- 764 74. **Wang, H. and D. P. Raleigh.** 2014. General amyloid inhibitors? A critical examination of the
765 inhibition of IAPP amyloid formation by inositol stereoisomers. *PLoS.One.* **9**:e104023.
766 doi:10.1371/journal.pone.0104023 [doi];PONE-D-14-14660 [pii].
- 767 75. **Wessels, D., D. F. Lusche, A. Scherer, S. Kuhl, M. A. Myre, and D. R. Soll.** 2014. Huntingtin
768 regulates Ca²⁺ chemotaxis and K⁺-facilitated cAMP chemotaxis, in conjunction with the
769 monovalent cation/H⁺ exchanger Nhe1, in a model developmental system: insights into its
770 possible role in Huntingtons disease. *Dev.Biol.* **394**:24-38. doi:S0012-1606(14)00400-X
771 [pii];10.1016/j.ydbio.2014.08.009 [doi].
- 772 76. **Williams, R. S. B., L. Cheng, A. W. Mudge, and A. J. Harwood.** 2002. A common mechanism of
773 action for three mood-stabilizing drugs. *Nature* **417**:292-295.
- 774 77. **Williams, R. S. B., W. J. Ryves, E. C. Dalton, B. Eickholt, G. Shaltiel, G. Agam, and A. J.**
775 **Harwood.** 2005. A molecular cell biology of lithium. *Biochem.Soc.Trans.* **32**:799-802.

776
777
778

779 **FIGURE 1. Inositol Signalling, and the Conservation of the Ino1 Protein in**
780 ***Dictyostelium* and Humans.** (A) Inositol metabolism. Ino1 converts glucose 6-phosphate to
781 inositol-3-phosphate, which is a rate-limiting step in inositol production. (B) Sequence
782 homology between the human (Q9NPH2-1) and *Dictyostelium* (Q54N49) Ino1 is present
783 throughout the proteins. Identical amino acids are shown in dark blue. The NAD binding and
784 catalytic domains are among the four regions that are highly conserved in eukaryotic Ino1
785 proteins: GWGGNNG (yellow), LWTANTERY (blue), SYNHLGNNDG (green) and
786 NGSPQNTFVPL (purple). The tetramerisation domain containing a putative catalytic site
787 (with the conserved amino acid residues SYNHLGNNDG) is shown in red. The amino acids
788 that were ablated in *Dictyostelium* Ino1 are shown by the horizontal black line. (C)
789 Alignment of the conserved regions of Ino1 proteins from various species, where ‘*’ denotes
790 identity, ‘.’ high conservation, ‘.’ low conservation levels. (D) Schematic representation of
791 the strategy used to prepare the *ino1* knock-out construct. N- and C-terminal portions of the
792 *ino1* gene were cloned into knock-out vector flanking blasticidin resistance (*bsr*) gene and the
793 knock-out cassette was transformed into *Dictyostelium* cells, where homologous
794 recombination deleted a portion of the *ino1* gene and disrupts the open reading frame. (E)
795 PCR screening strategy to identify *ino1* mutants, showing primers locations for genomic and
796 vector controls, the diagnostic knock-out product, and spanning the inserted *bsr* gene present
797 in the *ino1* knock-out. (F) PCR results showing the ablation of part of the *ino1* gene in the
798 *ino1* mutant, in comparison to wild-type cells. Ino1 - inositol 3-phosphate synthase; IMPase -
799 inositol monophosphatase; IPPase - inositol polyphosphate 1-phosphatase; IP2 - inositol
800 bisphosphate; IP3 - inositol trisphosphate; PLC - phospholipase C; PI – phosphatidylinositol;
801 PIP - phosphatidylinositol phosphate; PIP2 - phosphatidylinositol bisphosphate; PIP3 -
802 phosphatidylinositol trisphosphate; *bsr* – blasticidin resistance gene; G – genomic control; V
803 – vector control; KO – knock-out; 5’ – region corresponding to the transcription initiation site

804 of the *ino1* gene; 3' -region corresponding to the transcription termination site of the *ino1*
805 gene

806

807 **FIGURE 2. Ablating *ino1* in *Dictyostelium* Causes Inositol Auxotrophy.** (A)
808 *Dictyostelium* cells grown in liquid medium show rapid growth up to a stationary phase (at
809 168h). Ablation of *ino1* blocks cell growth in the absence of exogenous inositol, with only
810 partial restoration of wild-type growth by the addition of either 300 μ M or 500 μ M inositol.
811 (B) During starvation, wild-type *Dictyostelium* forms fruiting bodies without inositol pre-
812 treatment. Under the same conditions, *ino1*⁻ cells are unable to form fruiting bodies. Fruiting
813 body formation in *ino1*⁻ cells is restored when the cells are grown with inositol
814 supplementation prior to the assay. (C) Expressing *ino1-RFP* in *Dictyostelium ino1*⁻ cells was
815 confirmed by reverse transcription PCR (RT-PCR); with an *ig7* gene control, and Western blot
816 analysis to show the full length protein (with a ladder in kDa), that (D) restores growth rate
817 and (E) is present in the cytosol and (F) restores development in the absence of exogenous
818 inositol. (G) *ino1*⁻ cells are unable to grow on agar plates seeded with bacteria, and
819 expressing *ino1-RFP* in these cells restores bacterial growth. (A,D) statistical significance
820 was determined by a two-way ANOVA with Bonferroni post-test *** $p < 0.001$; error bars
821 represent S.E.M; experimental repeats = 3.

822

823 **FIGURE 3. Inositol Depletion Causes a Change in Velocity and Cell Shape, an**
824 **Activation of Autophagy, a Loss in Cell-Substrate Adhesion and a Reduction in**
825 **Cytokinesis in *Dictyostelium ino1*⁻ Cells.** (A) The level of *myo*-inositol analysed by NMR in
826 the wild-type and *ino1*⁻ cells grown with (+ 500 μ M) or without (-) exogenous inositol for 12
827 or 24 hours, or following inositol re-introduction (+/-) shown \pm S.E.M. Inositol levels were

828 reduced in the *ino1* mutant following inositol depletion for 12 and 24 hours, and restored to
829 basal levels following reintroduction for 12 hours. (B) Average velocity, aspect and
830 persistence of aggregation-competent *ino1* cells (grown with (+) 500 μ M inositol or without
831 (-) inositol for 24 hours prior to imaging) or wild-type cells during chemotaxis towards
832 cAMP. Velocity shows the distance travelled by cells over time. Aspect refers to the
833 roundness of cells (1 = perfectly round). Directness is a ratio of the distance travelled by a
834 cell compared to the total direct distance, where 1 represents a straight line. (C)
835 Autophagosomes were visualised in wild-type and *ino1* cells expressing Atg8-GFP and (D)
836 quantified in the presence or absence (24 hours) of inositol treatment. (E) Cell adhesion was
837 monitored in wild-type and *ino1* cells, and in *ino1* cells expressing *ino1*-RFP, in the
838 presence (500 μ M) and absence of inositol for at least 24 hours. (F) Cytokinesis was
839 examined in wild-type and *ino1* cells, and in *ino1* cells expressing *ino1*-RFP, using DAPI
840 nuclear stain to label cell nuclei, and (G) the number of nuclei per cell was quantified.
841 Statistical significance was determined by (A&B,D,E) an unpaired two-tailed *t*-test, where in
842 (A&B,D) each condition was compared separately to the wild-type (-inositol) and (D) *ino1*
843 (+inositol); (E,G) 2-way ANOVA with Bonferroni post-test, **p* < 0.05, ***p* < 0.01, ****p* <
844 0.001; error bars represent S.E.M; (A) experimental repeats = 4; (B) $n \geq 20$ cells analysed per
845 condition in 3 experimental repeats; (D) $n \geq 117$ cells analysed per condition in 3
846 experimental repeats; (E) experimental repeats = 3; (G) $n \geq 386$ cells analysed per condition
847 in 3 experimental repeats.

848

849 **FIGURE 4. Inositol Depletion Affects Phosphoinositides Levels in *Dictyostelium*.** (A) The
850 structure of phosphoinositol showing diacyl or ether/acyl fatty acid linkages to a glycerol
851 backbone and inositol head group. (B) Metabolic pathway depicting phospholipid production
852 from phosphatidic acid (PA) as an example. (C-Q) To monitor phospholipids in wild-type

853 and the *ino1⁻* mutant, cells were grown in the presence of inositol (500 μ M, denoted '+'), or
854 with inositol followed by inositol withdrawal (for 12 or 24h; denoted '+/-') or with inositol
855 added after a 24h depletion period (500 μ M for 12h; denoted '+/-/+') and control denotes
856 without inositol supplementation. The levels of ether/acyl (C34:1ea) or diacyl (C36:3aa)
857 phospholipids are shown as a percentage relative to phospholipid levels present in the wild-
858 type strain grown in the absence of inositol. Inositol depletion reduced the levels of diacyl PI,
859 PIP and PIP2 phosphoinositides; the level of PIP3 was undetectable, and reduced the levels
860 of ether/acyl PIP and PIP3. Statistical analysis was carried out comparing two groups at a
861 time: wild-type (+ inositol) vs *ino1⁻* (+ inositol), wild-type (+ inositol) vs *ino1⁻* (+/- 12 hour
862 inositol), wild-type (+ inositol) vs *ino1⁻* (+/- 24 hour inositol), and wild-type (+ inositol) vs
863 *ino1⁻* (+/-24 hour/+12 hour inositol) by unpaired two-tailed *t*-test to illustrate the significance
864 of changes due to the loss of the Ino1 protein, shown as “*”, **p* < 0.05, ***p* < 0.01, ****p* <
865 0.001; error bars represent S.E.M.; experimental repeats = 3.

866

867 **FIGURE 5. Comparison of Metabolic Profiles of *Dictyostelium* Following Ino1 Loss and**
868 **Inositol Depletion.** To monitor metabolic profiles in the wild-type and the *ino1⁻* mutant, cells
869 were grown in the presence of inositol (500 μ M, denoted '+'), or with inositol followed by
870 inositol withdrawal (12 or 24h; denoted '+/-') or with inositol added after a 24h depletion
871 period (500 μ M for 12h; denoted '+/-/+'), and control denotes without inositol
872 supplementation. (A) Metabolic variations existing between cell type and *myo*-inositol
873 exposure were assessed by principal component analysis (PCA) generated from the ¹H-NMR
874 spectra of the *Dictyostelium* metabolic fingerprints. The main source of variation (53%) was
875 driven by the mutation while inositol depletion accounted for approximately 12% of the
876 metabolic variation in this dataset. (B) Loadings plot associated with PC1 (red peaks pointing

877 upwards are positively associated with PC1 while those pointing downwards are negatively
878 associated with PC1). (C) Loadings plot associated with PC2. Experimental repeats = 5

879

880 **FIGURE 6. Metabolic profile analysis of the *inoI* mutant.** Cells were grown in the
881 presence of inositol (500 μ M, denoted '+'), or with inositol followed by inositol withdrawal
882 (12 or 24h; denoted '+/-') or with inositol added after a 24h depletion period (500 μ M for
883 12h; denoted '+/-/+'). (A,B) Metabolic changes induced by *inoI* ablation. Orthogonal
884 projection to latent structure discriminant analysis (O-PLS DA) was used in order to
885 determine the specific impact of the mutation on cell metabolism. (A) Plot of the scores
886 against the cross-validated scores generated by the O-PLS DA ($R^2Y = 0.89$, $Q^2 = 0.88$ and p
887 value for 500 random permutations = 0.002) using the $^1\text{H-NMR}$ spectra of the *Dictyostelium*
888 wild-type and *inoI* cells (except +/-24/+12h inositol exposure) as a matrix of independent
889 variables and mutation as predictor. (B) Loadings plot of the O-PLS DA model (peaks in red
890 indicate increased metabolite levels in response to the mutation). (C,D) Effect of inositol
891 treatment on the metabolism of the *inoI* mutant. (C) Plot of the scores against the cross-
892 validated scores generated by the O-PLS DA ($R^2Y = 0.67$, $Q^2Y = 0.51$ and p value for 500
893 permutations = 0.002) using the $^1\text{H-NMR}$ spectra of the *inoI* cells (-12h and -24h inositol vs
894 + inositol) as a matrix of independent variables and depletion of *myo*-inositol as a predictor.
895 (D) Loadings plot of the O-PLS DA model (peaks in red indicate increased metabolite levels
896 in response to the presence of inositol). (E,F) Reintroduction of *myo*-inositol post deprivation
897 induces a metabolic shift. (E) Plot of the scores against the cross-validated scores generated
898 by the O-PLS DA ($R^2Y = 0.90$, $Q^2Y = 0.86$ and p value for 500 permutations = 0.002) using
899 the $^1\text{H-NMR}$ spectra of the *inoI* cells (-12h and -24h inositol vs +/-/+ inositol) as a matrix of
900 independent variables and *myo*-inositol reintroduction as a predictor. (F) Loadings plot of the

901 O-PLS DA model (peaks in red indicate increased metabolite levels in response to the
902 depletion of *myo*-inositol), Experimental repeats = 4.

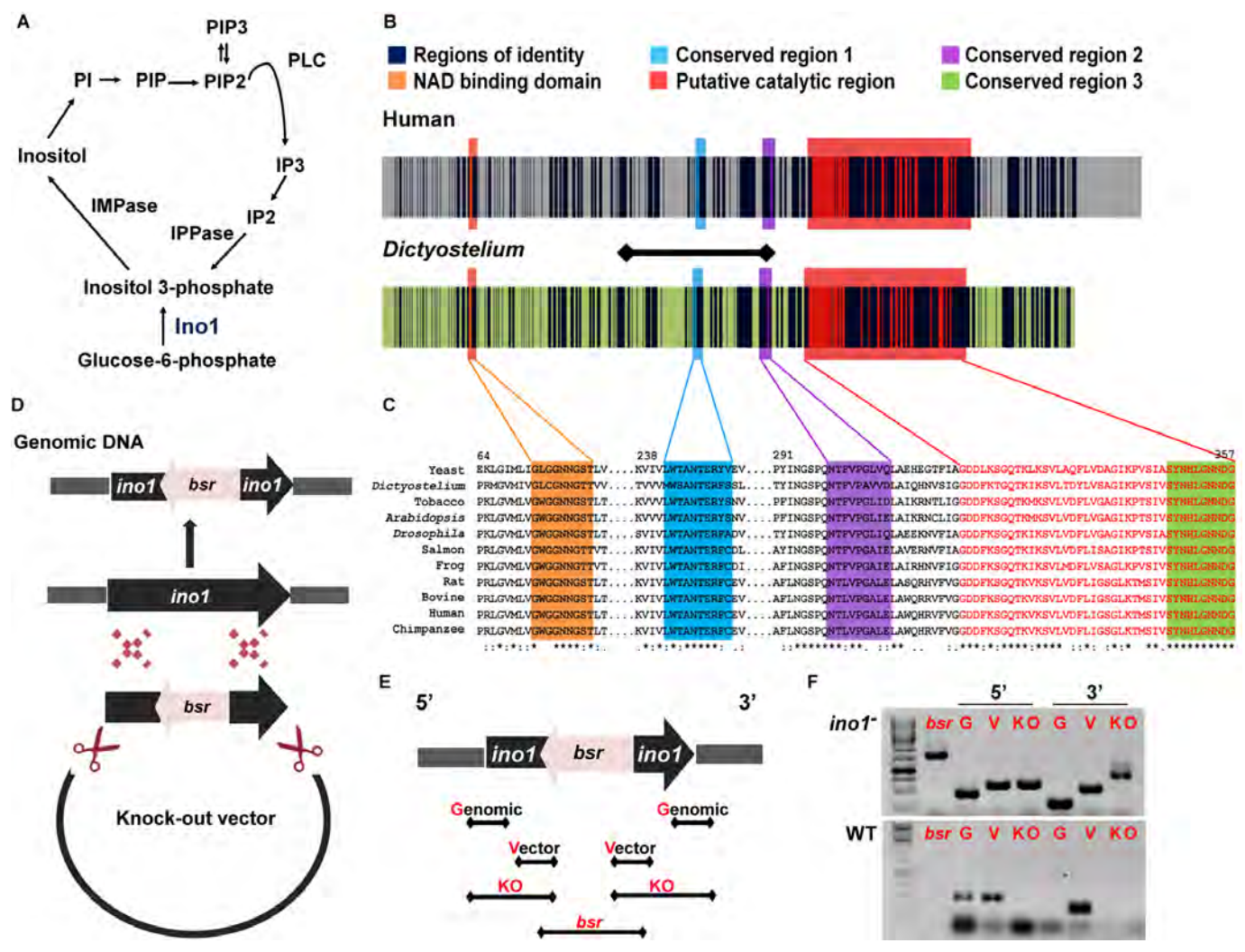
903

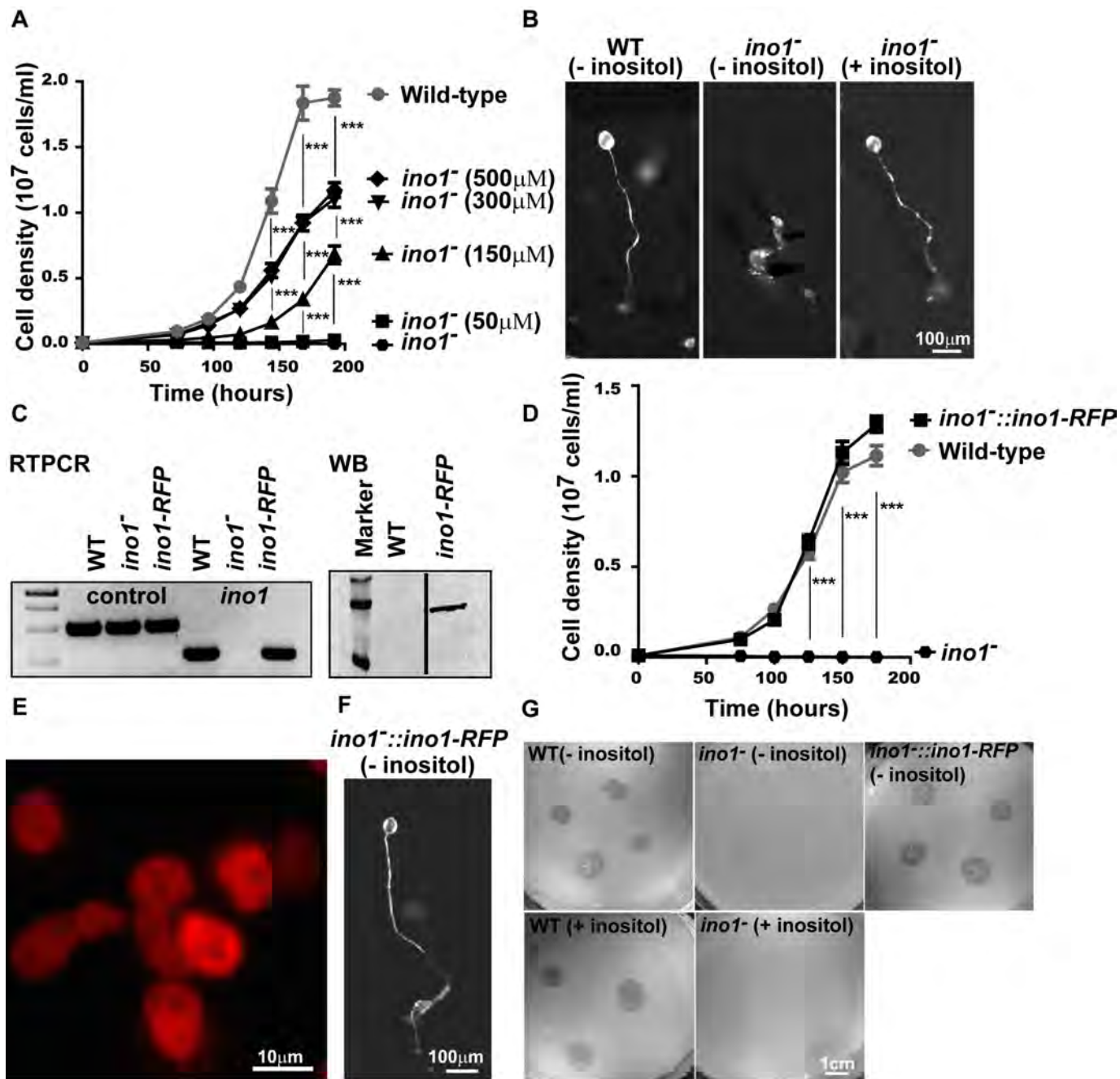
904 **FIGURE 7. Levels of metabolites in wild-type and *inoI* cells grown under varying**
905 **inositol conditions.** Metabolite levels, measured by NMR, were quantified using MATLAB
906 and plotted to illustrate changes observed in wild-type and *inoI* cells for (A) amino acids (B)
907 cell cycle and DNA-related metabolites (C) other metabolites. Control denotes without
908 inositol supplementation. Statistical analysis was carried out between two groups: wild-type
909 (AX2) (+ inositol) vs. *inoI* (+ inositol) by unpaired two-tailed *t*-test to illustrate the
910 significance of changes due to the loss of Ino1 protein, shown as “*”, **p* < 0.05, ***p* < 0.01,
911 ****p* < 0.001. A separate unpaired two-tailed *t*-test analysis was used to compare two groups:
912 *inoI* (+ inositol) vs. *inoI* (- inositol 12h) and *inoI* (+ inositol) vs. *inoI* (- inositol 24h),
913 shown as “^{ct+}”, ⁺*p* < 0.05, ⁺⁺*p* < 0.01, ⁺⁺⁺*p* < 0.001; error bars represent S.E.M.; experimental
914 repeats = 5 per sample/per condition.

915

916 **FIGURE 8. An Ino1 non-catalytic role in *Dictyostelium*.** (A) Ino1-RFP protein with an
917 aspartic acid to alanine substitution (*ino1D342A*) in a highly conserved region of a catalytic
918 domain was overexpressed in the wild-type and *inoI* cells. In the *inoI* cells, the mutated
919 protein was unable to rescue the *inoI* inositol auxotrophy, consistent with a catalytically
920 inactive protein. In the wild-type cells, expressing the mutant protein significantly decreased
921 growth, while the addition of exogenous inositol partially rescued this phenotype.. Statistical
922 analysis was carried out for each individual condition compared to wild-type (AX2) by
923 unpaired two-tailed *t*-test, **p* < 0.05, ****p* < 0.001; error bars represent S.E.M.; experimental
924 repeats = 3 (B) Co-immunoprecipitation of the Ino1-RFP protein (or RFP only control)

925 expressed in *ino1⁻* cells, using anti-RFP coated beads, shown for bound (B) and non-bound
926 fractions (NB). SDS-PAGE gels were visualised following Coomassie staining (left) and
927 analysed by Western blot with an anti-RFP antibody (right). Bands specific to Ino1-RFP (and
928 absent from the RFP control) were analysed by mass spectrometry to identify potential Ino1
929 binding partners. (C) FLAG-tagged potential interacting proteins GpmA, PefB, and Q54IX5,
930 were investigated by immunoprecipitation using Ino1-RFP and anti-RFP-coated beads,
931 followed by Western blot analysis with anti-RFP and anti-FLAG antibodies. (D) An Ino1-
932 Q54IX5 interaction was confirmed by immunoprecipitation of the GFP-Q54IX5 protein with
933 anti-GFP-coated beads in the presence of Ino1-RFP (or RFP only) and Western blot analysis
934 with anti-RFP and anti-GFP antibodies.



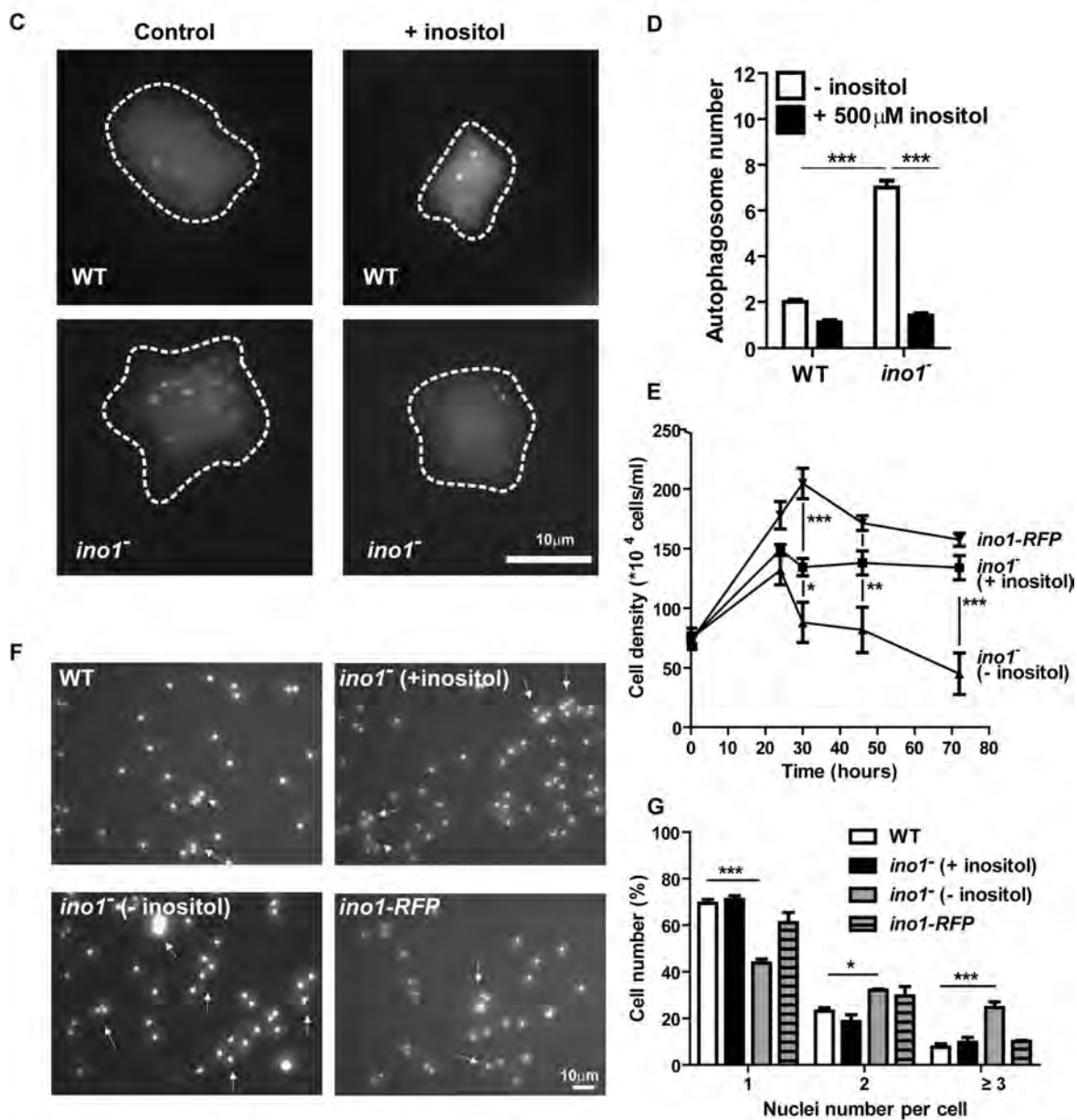


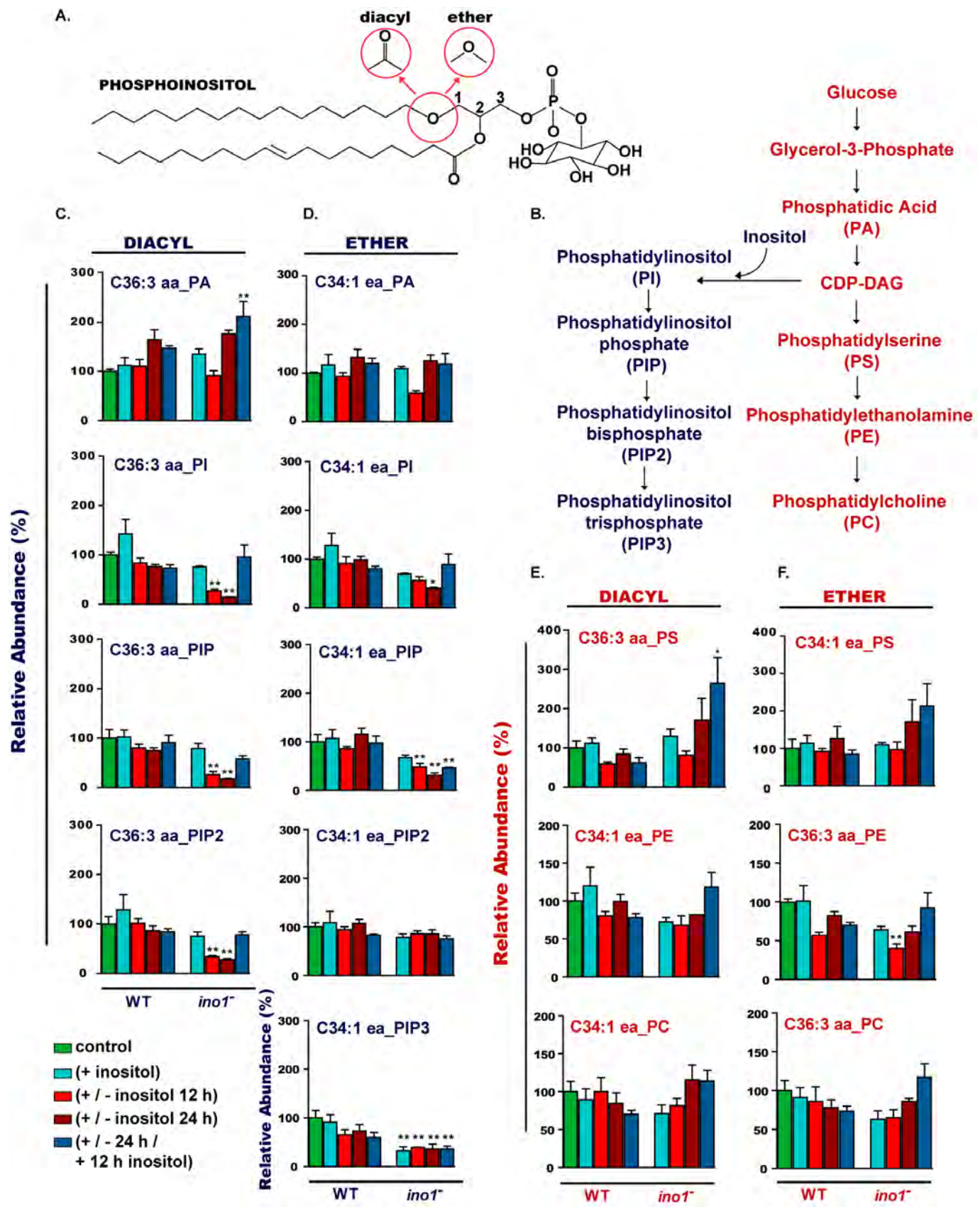
A

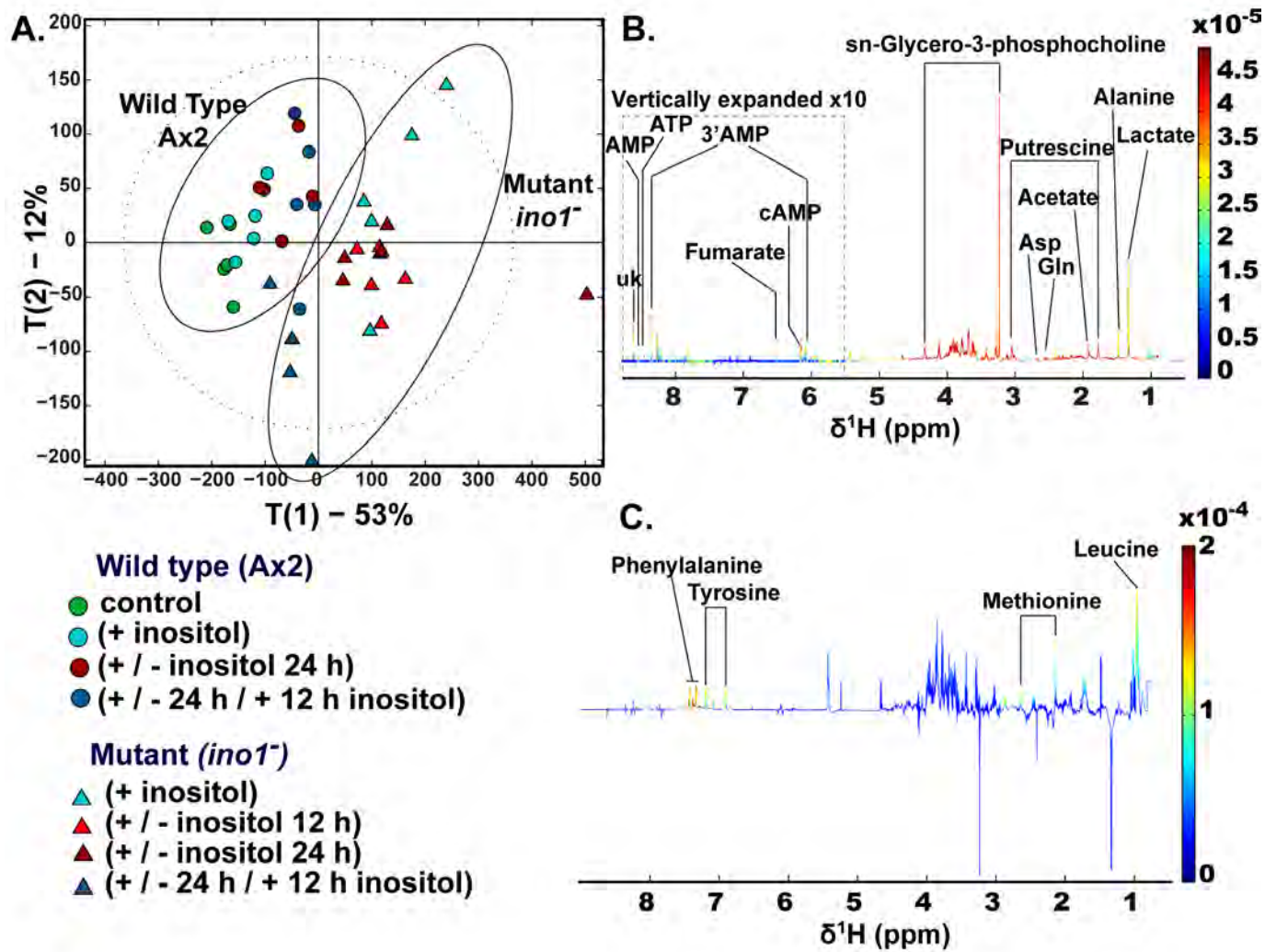
Cell Line	Treatment	Concentration (μM)
	(500 μM inositol)	<i>myo</i> -inositol
WT (Ax2)	(-)	1.47 ± 0.12
	(+)	$3.40 \pm 0.16^{***}$
	(- 24 h)	1.60 ± 0.23
	(+/-12 h /+ 24h)	2.17 ± 0.22
<i>ino1</i> ⁻	(+)	1.82 ± 0.22
	(- 12 h)	$0.80 \pm 0.13^{**}$
	(- 24 h)	1.15 ± 0.10
	(+/-12 h /+ 24h)	1.96 ± 0.41

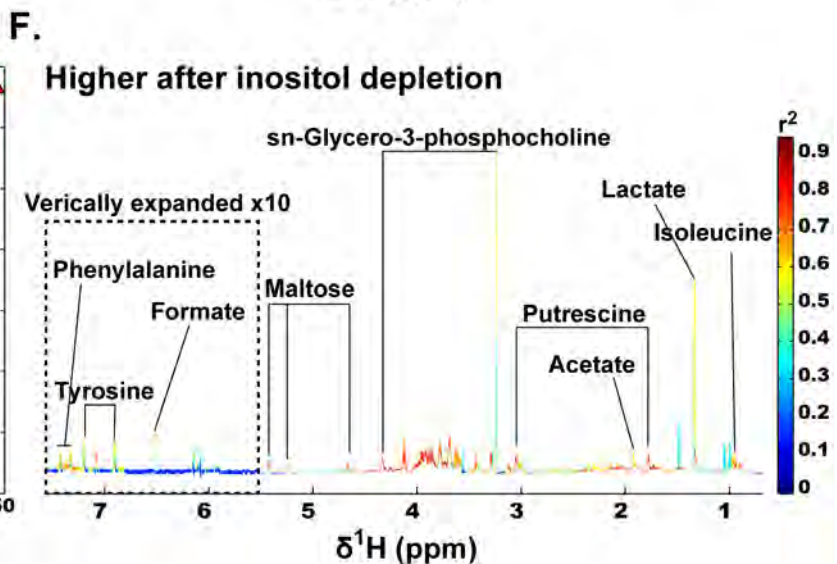
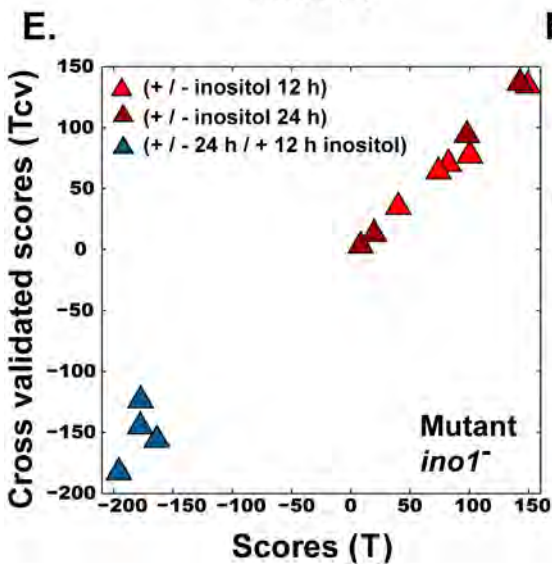
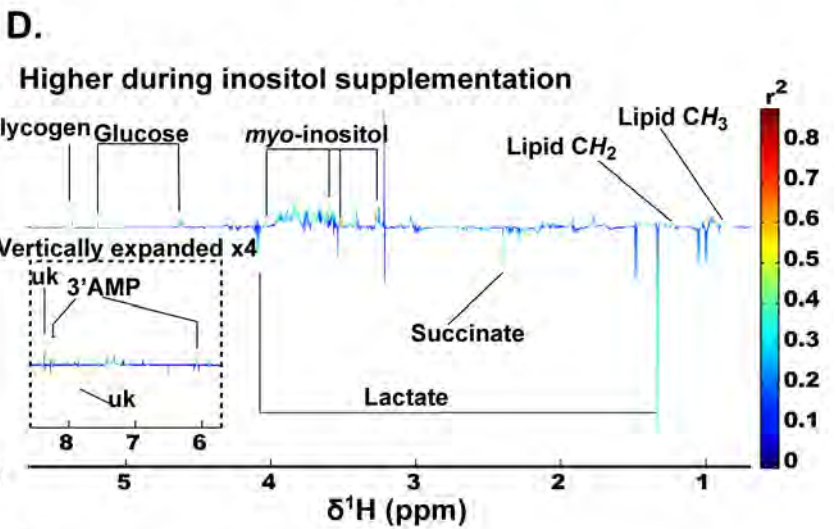
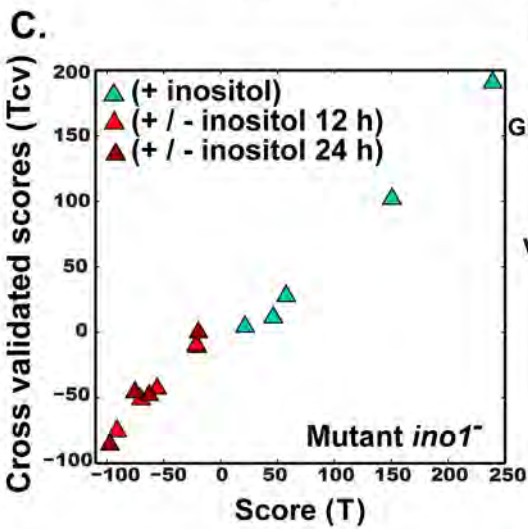
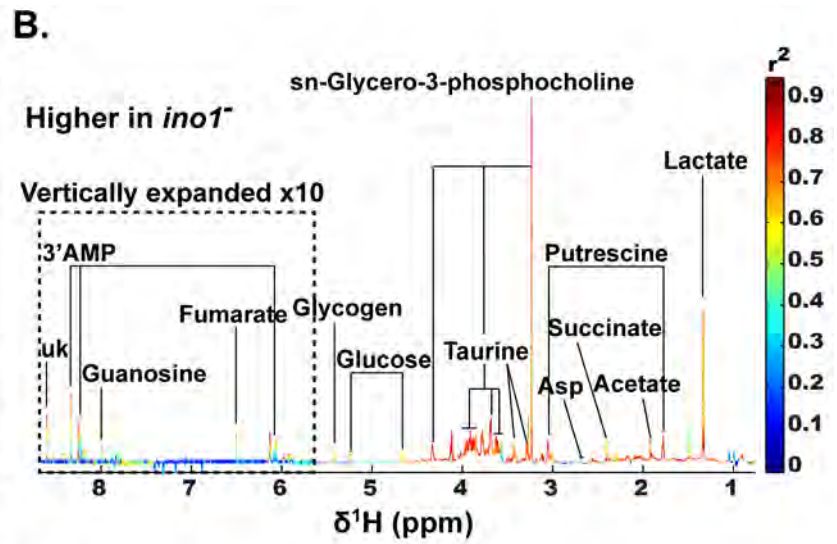
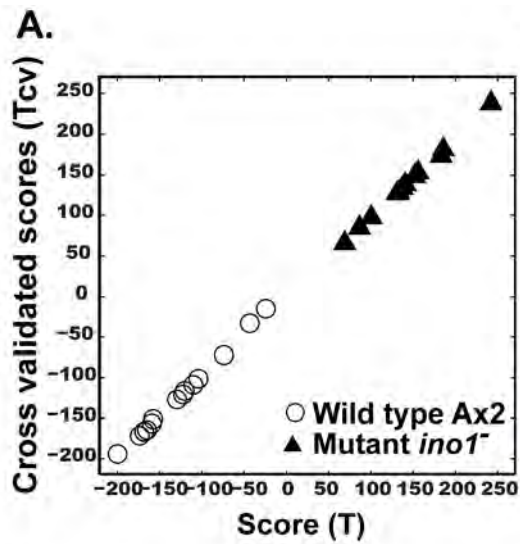
B

Cell Line	Velocity ($\mu\text{m}/\text{min}$)	Aspect	Directness
WT (Ax2)	9.63 ± 1.49	2.96 ± 0.61	0.87 ± 0.14
<i>ino1</i> ⁻ (- inositol)	$4.97 \pm 1.18^{***}$	$1.76 \pm 0.46^{***}$	$1.68 \pm 0.46^*$
<i>ino1</i> ⁻ (+ inositol)	7.42 ± 3.32	$1.63 \pm 0.55^{***}$	1.12 ± 0.54

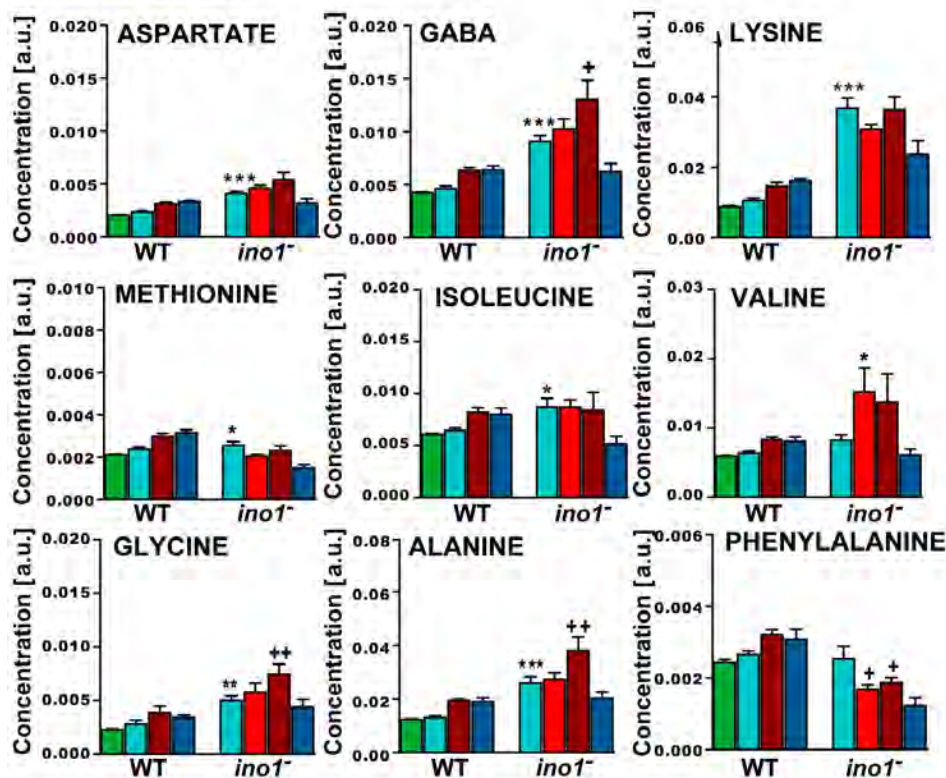




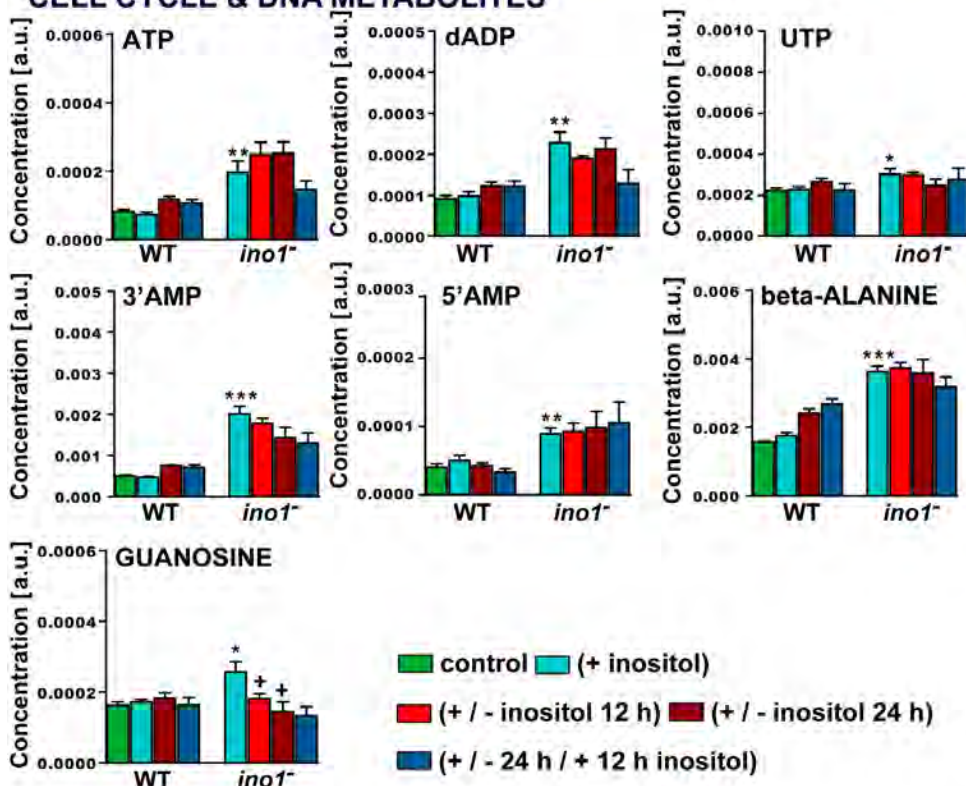




A. AMINO ACIDS



B. CELL CYCLE & DNA METABOLITES



C. OTHER METABOLITES

